

Uloga polifosfata u prilagodbi cijanobakterije *Synechocystis* sp. PCC 6803 na klorozu uzrokovanu nedostatkom dušika

Janović, Ana

Master's thesis / Diplomski rad

2021

Degree Grantor / Ustanova koja je dodijelila akademski / stručni stupanj: **University of Zagreb, Faculty of Science / Sveučilište u Zagrebu, Prirodoslovno-matematički fakultet**

Permanent link / Trajna poveznica: <https://um.nsk.hr/um:nbn:hr:217:655797>

Rights / Prava: [In copyright](#) / [Zaštićeno autorskim pravom.](#)

Download date / Datum preuzimanja: **2024-09-28**



Repository / Repozitorij:

[Repository of the Faculty of Science - University of Zagreb](#)



University of Zagreb
Faculty of Science
Department of Biology

Ana Janović

The role of polyphosphate in adaptation to nitrogen starvation-
induced chlorosis in cyanobacterium *Synechocystis* sp. PCC 6803

Graduation Thesis

Zagreb, 2021

Sveučilište u Zagrebu
Prirodoslovno-matematički fakultet
Biološki odsjek

Ana Janović

Uloga polifosfata u prilagodbi cijanobakterije *Synechocystis* sp. PCC
6803 na klorozu uzrokovanu nedostatkom dušika

Diplomski rad

Zagreb, 2021

This graduation thesis was conducted at the University of Tübingen – Faculty of Biology, Interfaculty Institute for Microbiology and Infection Medicine Tübingen, Tübingen, Germany, under supervision of Prof. Dr. Karl Forchhammer. The thesis was submitted for evaluation to the Department of Biology at the Faculty of Science, University of Zagreb in order to obtain the title of Master of Molecular Biology (mag. biol. mol.).

Acknowledgements

“Šta ne boli – to nije život; šta ne prolazi – to nije sreća.”

“What doesn't hurt - is not life; what doesn't pass - is not happiness.”

Ivo Andrić

I must thank Prof. Dr. Karl Forchhammer who gave me an opportunity to work in his laboratory during period of ten months. His office's door always remained opened for me when facing hurdles and doubts. In those moments his advice was always on point and, motivating and, most importantly led to improvements of my experiments.

I must thank Sofía Doello Román, a PhD student and my direct supervisor in the lab who always had enough patience and encouragement for me. She introduced me to most of the lab techniques I used and helped me to develop myself as a researcher.

As well, I would like to thank all other members of the Forchhammer's group who proved to be extremely helpful, benevolent and provided a nice atmosphere in the lab, despite the difficult times.

I would like to thank my family for their care and support and for enabling me to completely focus on my studies during the last five years.

I would like to thank my friends for their support and all the nice moments during my college days.

I would like to thank to Dr. Željka Vidaković-Cifrek, Assoc. Prof. for reading this Master Thesis and the helpful comments she provided.

I would like to thank Erasmus Office from The University of Zagreb for the financial support of my stay in Tübingen.

BASIC DOCUMENTATION CARD

University of Zagreb

Faculty of Science

Department of Biology

Graduation Thesis

THE ROLE OF POLYPHOSPHATE IN ADAPTATION TO NITROGEN STARVATION-INDUCED CHLOROSIS IN CYANOBACTERIUM *SYNECHOCYSTIS*

SP. PCC 6803

Ana Janović

Rooseveltova trg 6, 10000 Zagreb, Croatia

Polyphosphate is a type of storage polymer consisting of phosphate residues connected by phosphoanhydric bonds. It is synthesized by polyphosphate kinase enzyme (PPK) from ATP in prokaryotes. Microbes tend to accumulate polyphosphate in stressful conditions such as nutrient-deprivation. *Synechocystis* sp. PCC 6803 is a model organism for photosynthetic unicellular cyanobacteria that do not fix nitrogen. Its adaptation to nitrogen-induced chlorosis has been extensively studied and is well characterized. The major role in this process has been glycogen - a polymer that accumulates in nitrogen deprivation and serves as an energy source during recovery from nitrogen starvation. The role of polyphosphate has not been widely investigated in *Synechocystis* and other cyanobacteria. In this thesis, the role of polyphosphate was studied on polyphosphate kinase-deficient mutant (*ppk*). Inactivation of *ppk* didn't affect normal growth. *ppk* mutant shows highly impaired recovery from nitrogen starvation. Polyphosphate seems to be important for energy metabolism judged by elevated ATP levels in *ppk* mutant. A protocol for absolute quantification of polyphosphate based on phenol-chloroform extraction and ethanol precipitation followed by enzymatic digestion of polyphosphate has been adapted for *Synechocystis* sp. PCC 6803. As well, PPK1 enzyme has been purified and characterized. PPK1 shows allosteric dependence on inorganic phosphate.

(47 pages, 21 figures, 4 tables, 72 references, original in: English)

Thesis is deposited in the Central Biological Library

Keywords: *Synechocystis* sp. PCC 6803, polyphosphate, nitrogen starvation, polyphosphate kinase, cyanobacteria

Supervisor: Dr. Karl Forchhammer, Prof.

Cosupervisor: Dr. Željka Vidaković-Cifrek, Assoc. Prof.

Reviewers: Željka Vidaković-Cifrek, Assoc. Prof., Dr. Marin Ježić, Asst. Prof.,

Dr. Nenad Malenica, Asst. Prof., Dr. Petra Peharec Štefanić, Asst. Prof

Thesis accepted: 11/01/2021

TEMELJNA DOKUMENTACIJSKA KARTICA

Sveučilište u Zagrebu

Prirodoslovno-matematički fakultet

Biološki odsjek

Diplomski rad

ULOGA POLIFOSFATA U PRILAGODBI CIJANOBakterIJE *SYNECHOCYSTIS* SP. PCC 6803 NA KLOROZU UZROKOVANU NEDOSTATKOM DUŠIKA

Ana Janović

Rooseveltov trg 6, 10000 Zagreb

Polifosfat je pričuvni polimer koji se sastoji od fosfatnih monomera povezanih fosfoanhidridnim vezama. U prokariota sintetizira se iz ATP-a pomoću enzima polifosfat kinaze (PPK). Mikroorganizmi akumuliraju polifosfat u stresnim uvjetima poput nedostatka hranjivih tvari. *Synechocystis* sp. PCC 6803 modelni je organizam za proučavanje fotosintetskih jednostaničnih cijanobakterija koje nemaju sposobnost fiksacije dušika. Njegova prilagodba na klorozu uzrokovanu nedostatkom dušika je temeljito opisana. Glavnu ulogu u ovome procesu ima polimer glikogen koji se akumulira tijekom adaptacije na nedostatak dušika i služi kao izvor energije prilikom izlaska iz dormantnog stanja. Uloga polifosfata kod ove i ostalih vrsta cijanobakterija nije mnogo istražena. U okviru ovog diplomskog rada, proučavana je uloga polifosfata na mutantu za polifosfat kinazu (*ppk*). Inaktivacija gena *ppk* ne utječe na normalni rast cijanobakterije *Synechocystis*. Mutant za gen *ppk* ima smanjenu sposobnost izlaska iz dormantnog stanja izazvanog nedostatkom dušika. Polifosfat vjerojatno ima uloga u energetske metabolizmu stanice na što ukazuje povećana razina ATP-a kod *ppk* mutanta. Protokol za apsolutnu kvantifikaciju polifosfata na temelju izolacije fenol-kloroformom i precipitacije etanolom nakon koje slijedi enzimska razgradnja polifosfata prilagođen je za cijanobakteriju *Synechocystis* sp. PCC 6803. Enzim PPK1 iz cijanobakterije *Synechocystis* izoliran je i karakteriziran. PPK1 pokazuje alosteričku ovisnost o anorganskom fosfatu.

(47 stranica, 21 slika, 4 tablice, 72 literaturna navoda, jezik izvornika: engleski)

Rad je pohranjen u: Središnjoj biološkoj knjižnici

Ključne riječi: *Synechocystis* sp. PCC 6803, polifosfat, nedostatak dušika, polifosfat kinaza, cijanobakterije

Voditelj: Dr. sc. Karl Forchhammer, prof.

Suvoditelj: Dr. sc. Željka Vidaković-Cifrek, izv. prof.

Ocjenitelji: Izv. prof. dr. sc. Željka Vidaković-Cifrek, Doc. dr.sc. Marin Ježić,

Doc. dr. sc. Nenad Malenica, Doc. dr. sc. Petra Peharec Štefanić

Rad prihvaćen: 11/01/2021

TABLE OF CONTENTS

1. INTRODUCTION.....	1
1.1. Polyphosphate as a prokaryotic polymer.....	1
1.2. Quantification of polyphosphate.....	2
1.3. The role of polyphosphate in microorganisms	3
1.4. Polyphosphate in cyanobacteria and <i>Synechocystis</i> PCC 6803	5
1.5. Bacterial dormancy as a survival strategy	6
1.6. <i>Synechocystis</i> PCC 6803 as a model organism for the study of nitrogen-induced chlorosis	7
2. THE AIM OF THESIS.....	10
3. MATERIALS AND METHODS	11
3.1. Cultivation of cyanobacterial cultures	11
3.2. Visualisation of polyphosphate in <i>Synechocystis</i> using DAPI	11
3.3. Segregation check of <i>ppk</i>	12
3.4. Quantification of polyphosphate in <i>Synechocystis</i>	13
3.5. Quantification of glycogen in <i>Synechocystis</i>	14
3.6. Quantification of ATP and ADP levels in <i>Synechocystis</i>	14
3.7. Quantification of polyhydroxybutyrate in <i>Synechocystis</i>	15
3.8. Spot-agar assay	15
3.9. Purification of PPX1 from <i>S. cerevisiae</i>	15
3.10. Cloning of PPK1 from <i>Synechocystis</i>	16
3.11. Purification of recombinant PPK1	17
3.12. Determination of polyphosphate-synthesizing activity of PPK1.....	18
3.13. Determination of polyphosphate-degrading activity of PPK1.....	19
4. RESULTS	20
4.1. Visualization of polyphosphate granules in <i>ppk</i> mutant, exponentially growing cultures, chlorosis and resuscitation.....	20
4.2. Spot-agar assay of <i>ppk</i> and WT cultures	22
4.3. Polyphosphate quantification in <i>Synechocystis</i>	24
4.3.1. Optimization of protocol for polyphosphate quantification in <i>Synechocystis</i>	24
4.3.2. Polyphosphate levels during chlorosis and resuscitation	26
4.4. Comparison of glycogen synthesis and degradation in WT and <i>ppk</i> during chlorosis and resuscitation	27
4.5. ATP levels in resuscitation and upon entry in nitrogen-induced starvation.....	28
4.6. PHB content of <i>ppk</i> and WT	30
4.7.1. Purification of PPK1 protein	31
4.7.2. Polyphosphate-synthesizing activity of PPK1 from <i>Synechocystis</i>	31

4.7.3. Polyphosphate-degrading activity of PPK1 from <i>Synechocystis</i>	34
5. DISCUSSION	35
6. CONCLUSION	40
7. REFERENCES.....	41
APPENDIX.....	46
CURRICULUM VITAE.....	IV

Abbreviations

ADP – adenosine diphosphate	NADH – nicotinamide adenine dinucleotide (reduced)
AMP – adenosine monophosphate	NADPH – nicotinamide adenine dinucleotide phosphate
ATP – adenosine triphosphate	Ni-NTA – nickel-nitriloacetic acid
BP – band-pass	OD – optical density
BSA – bovine serum albumin	PBS – phosphate-buffered saline
CDW – cell dry weight	PCR – polymerase chain reaction
DAPI – 4',6-diamidino-2-phenylindole	PEG – polyethylene glycol
dNTP – deoxynucleotide triphosphate	PEP – phosphoenolpyruvate
DTT – dithiothreitol	PGM – phosphoglucomutase
EDTA – ethylenediaminetetraacetic acid	PHB – polyhydroxybutyrate
EG – exponential growth	Pi – inorganic phosphate
fw – forward	PK – pyruvate kinase
G6PDH – glucose-6-phosphate-dehydrogenase	PMSF – phenylmethylsulfonyl fluoride
GDP – guanosine diphosphate	polyP – polyphosphate
GS-GOGAT – glutamin-synthetase/ glutamin-oxoglutarat-aminotransferase	PPK – polyphosphate kinase
GTP – guanosine triphosphate	PPX – exopolyphosphatase
HEPES – 4-(2-hydroxyethyl)-1-piperazineethanesulfonic acid	rev – reverse
HK – hexokinase	RLU – relative light unit
HPLC – high performance liquid chromatography	RT - room temperature
IPTG – isopropyl β -d-1-thiogalactopyranoside	rpm – rounds per minute
LB – Luria-Bertani	SDS-PAGE – sodium dodecyl sulphate-polyacrylamide gel electrophoresis
LDH – lactate dehydrogenase	TCA – tricarboxylic acid
LP – longpass	Tris – trisaminomethane
NAD – nicotinamide adenine dinucleotide (oxidized)	TE – Tris-EDTA
	WGS – whole-genome sequencing
	WT – wild type

1. INTRODUCTION

1.1. Polyphosphate as a prokaryotic polymer

Microorganisms produce various types of biopolymers, the most common being glycogen, cyanophycin, polyhydroxybutyrate (PHB), cellulose and polyphosphate (polyP) (Rehm, 2010). Synthesis and degradation of different polymers are a part of bacterial stress response and the lack of them severely affects ability to adapt and recover from unfavourable conditions (Damrow et al., 2016).

Polyphosphate is a type of polymer consisting of inorganic phosphate chain of up to 1000 monomers linked by covalent bonds. Homologs for enzymes involved in synthesis and degradation of polyP have been found in different microbes (Brown & Kornberg, 2008). Polyphosphate kinase (PPK) is conserved among prokaryotes and was the first polyphosphate-associated protein to be characterized (Ahn & Kornberg, 1990). PPK is involved in the process of polyphosphate synthesis consuming ATP to elongate a polyphosphate chain. Another enzyme, exopolyphosphatase (PPX) is involved in a catalytic reaction of the hydrolysis of phosphoanhydridic bonds of polyphosphate chain while realising orthophosphate (Akiyama et al., 1993).

Main enzyme for polyphosphate synthesis among prokaryotes is polyphosphate kinase 1 (PPK1) that greatly favours anabolic reaction of polyphosphate synthesis with the highest affinity for ATP as a phosphate donor among triphosphonucleotides (Tzeng & Kornberg, 2000). Mutations in PPK1 in different microorganisms have been linked with various defects, such as in stress adaptation, normal growth, virulence and motility (Fraley et al., 2007). Its mechanism of polyP synthesis, regulation and structure was investigated in detail in *Escherichia coli* (Rao et al., 2009). Highly conserved among microorganism are two histidine side chains responsible for its catalytic activity by directly binding phosphate during catalysis (Kumble et al., 1996). Further, dimerization of the enzyme and its autophosphorylation are important for its polyP synthesizing activity (Kornberg et al., 1999). Activity of the enzyme has been shown to be dependent on concentrations of adenonucleotides ATP and ADP and as well on the presence of inorganic phosphate and polyphosphate in some microorganisms (Robinson & Wood, 1986). In the conditions of high concentrations of ADP and the presence of polyphosphate, PPK1 favours a polyphosphate-degrading reaction producing ATP from ADP, which doesn't seem to be of physiological relevance in most organisms. On the other hand, it is the other enzyme;

PPK2 which mainly serves as a polyphosphate-degrading enzyme favouring a reaction of polyP degradation where the phosphate is transferred to ADP, AMP, GDP or GMP, as shown in *Pseudomonas aeruginosa* (Zhang et al., 2002). As well, the same study observed that PPK2 favours shorter length polyP chains as a source of orthophosphate. Other less known reactions in which polyP may be involved in the cells include phosphate transferal from polyP by polyphosphate/ATP NAD kinase that may use both polyP and ATP for phosphorylation of NAD⁺. As well, polyphosphate may be used as a phosphate donor for glucose phosphorylation (Hsieh et al., 1993). Further, a study on *Mycobacterium tuberculosis* showed that this enzyme favours polyP over ATP as a phosphate donor (Kawai et al., 2000).

Cells store polyphosphate in terms of either soluble polyphosphate or granules that can be visualised by light microscope after DAPI staining and under electron microscope. As well, polyphosphate chain length distribution varies under different conditions (Klauth et al., 2006). Binding of polyphosphate granules to DAPI shifts its emission maximum to 525 nm enabling to differentiate between DAPI-DNA and DAPI-polyphosphate complex. Some bacteria form acidocalcisomes structures visible under the electron microscope consisting of polyphosphate surrounded by lipid membrane rich in proton pumps and calcium-transporters. Those acidic compartments serve as a storage of phosphate, basic amino acids and calcium (Docampo et al., 2010).

1.2. Quantification of polyphosphate

The main obstacle in studying the role of polyphosphate has been a lack of reliable quantification method.

Different methods would often yield highly dissimilar estimates of polyphosphate abundance due to losses in the extraction procedure and differences among quantification methods. Many extraction and detection methods were shown to be biased towards chain length of polyphosphate (Bru et al., 2017; Christ et al., 2020). Instead, quantification methods based on DAPI staining of a whole cell extract suffer from bias towards composition of the extract, as presence of other molecules capable of binding DAPI interfere with the measurement (Christ et al., 2020). On the other hand, methods relying on polyphosphate isolation prior to its quantification would often yield low amounts polyphosphate. Enzymatic methods rely on the usage of either recombinant PPK or PPX enzyme producing orthophosphate or ATP

respectively, which are being detected, thereby enabling absolute quantification of this polymer.

A quantification method based on phenol-chloroform extraction of polyphosphate followed by its precipitation by ethanol and degradation by purified PPX enzyme has become a *gold-standard* for polyphosphate determination among microorganisms (Bru et al., 2017). This method enables extraction of polyphosphate chains of various lengths. As well, usage of neutral phenol-chloroform prevents polyphosphate hydrolysis. Finally, total amount of polyphosphate is determined after colorimetric detection of phosphate released during hydrolysis of polyphosphate with purified PPX enzyme.

1.3. The role of polyphosphate in microorganisms

The role of polyphosphate has first been studied in *E. coli* where its accumulation was observed under stressful conditions, e.g. amino acid or nitrogen starvation and osmotic shock, while its degradation proceeded shortly after addition of the missing nutrient (Rao & Kornberg, 1996). A mutant deficient in PPK1 unable to produce polyphosphate chains demonstrated much lower ability to survive the stationary phase and greater sensitivity to oxidative and heat stress explained by the fact that the mutant is unable to produce RpoS sigma-factor important for stationary-phase adaptation (Ault-Riché et al., 1998). Early studies on polyphosphate accumulation under alkaline stress demonstrated its role in pH regulation in unicellular alga *Dunaliella salina* with polyphosphate degradation correlating with the recovery of cytoplasmic pH (Pick et al., 1990).

It has also been shown that polyphosphate is directly involved in transcriptional regulation through forming a complex with *E. coli* RNA polymerase sigma factor 70 (Kusano & Ishihama, 1997). Another research on *M. tuberculosis* showed that polyphosphate is important for induction of transcription of *sigE* gene involved in survival during oxidative stress. In this case, polyphosphate serves as a phosphate donor for phosphorylation and concomitant activation of *mrpA* transcription regulator (Sureka et al., 2007). Another way in which PolyP affects gene expression is by being a part of degradosome structure along with ribonuclease enzymes in *E. coli* where it is involved in inhibition of mRNA degradation (Hood et al., 2016).

Polyphosphate also serves as an inorganic phosphate storage, utilised under phosphate starvation. Expression of polyphosphate associated enzymes PPX and PPK has been shown to be under control of *pho*-regulon (Munévar et al., 2017) which is a negative regulator of the

expression of phosphate uptake genes. As well, higher polyphosphate levels were detected in *P. aeruginosa* as a consequence of *phoU* deletion (de Almeida et al., 2015).

During amino acid starvation polyphosphate is involved in the process of protein degradation providing the amino acids (Kuroda et al., 1997). Furthermore, it has been revealed that during this process polyphosphate forms a complex with Lon and Clp proteases followed by degradation of free ribosomal proteins (Kuroda et al., 2001). Apart from that, polyphosphate is able to compete along with DNA for binding with Lon protease possibly having an effect on degradation of DNA-binding transcription-regulating proteins (Nomura et al., 2004). Also, the process of polyphosphorylation of lysine residues plays a role in the ribosome biogenesis in *Saccharomyces cerevisiae* (Bentley-DeSousa et al., 2018).

A study of polyphosphate levels in 230 mutant strains of *S. cerevisiae* showed higher glycogen content among mutants with decreased levels of polyphosphate showing that polyphosphate impacts primary energy metabolism of the cell (Freimoser et al., 2006).

Another study demonstrated how polyphosphate is important for adaptation and survival during oxidative stress (McMeechan et al., 2007). The *ppk* mutant from this study also demonstrated elevated levels of ATP compared to the wild type. Further, the presence of polyphosphate seemed to alleviate protein unfolding under oxidative stress by a direct interaction with the damaged protein (Gray & Jakob, 2016).

Polyphosphate is additionally involved in the process of removal of toxic metals from the cell through their chelation followed by PPX mediated degradation of polyphosphate necessary for the heavy metal elimination from the cell (McMeechan et al., 2007).

Proteomic study on *E. coli ppk* mutant showed elevated levels of proteins involved in TCA (tricarboxylic acid cycle) cycle and beta-oxidation processes and also of chaperone proteins. Also, compared to *ppx* mutant, *ppk* exhibited oppositely regulated metabolic pathways with glycolytic and TCA cycle enzymes being upregulated and downregulated in *ppk* and *ppx* mutant respectively (Varas et al., 2017). Another proteomic study also showed higher levels of TCA cycle enzymes as well as highly overrepresented ATP-synthase subunits (Varela et al., 2010). These results, along with recorded higher ATP levels in the mutant suggest involvement of polyphosphate in the general energy metabolism of the cell.

Connection of polyphosphate accumulation and metabolism of polymer polyhydroxybutyrate has been proved in chemolithotrophic *Ralstonia eutropha*. It was demonstrated that polyphosphate over-accumulating mutants have decreased ability of utilising accumulated PHB

granules during stationary phase (Tumlirsch et al., 2015) . Besides, polyphosphate alongside PHB and calcium ions seem to be involved in the membrane pore formation that may have a role in transport of DNA and ions based on experiments studying effects of polyphosphate absence on bacterial competence (Reusch et al., 1995).

Polyphosphate has also been shown to have a role in the processes of cell cycle and division.

Synthesis of polyphosphate was proved to correlate with the cell cycle progression observed as an increase of polyphosphate granules' size before the cell division as well as in its positioning within the cell. Mutants disrupted in chromosome partition were as well unable to achieve proper localisation of polyphosphate granules in *Caulobacter crescentus* (Henry & Crosson, 2013).

Cell cycle control of *P. aeruginosa* also seems to be under control of polyP as its synthesis and localisation highly correlate with the cell cycle exit. Moreover, the mutants lacking polyphosphate have disrupted chromosomal replication (Racki et al., 2017).

1.4. Polyphosphate in cyanobacteria and *Synechocystis* PCC 6803

A small number of studies exist on the role of polyphosphate in *Synechocystis* species. Transmission microscopy images of *Synechocystis* detected on average zero to three polyphosphate bodies per cell, with polyphosphate bodies often being in proximity of carboxysomes (Nierzwicki Bauer et al., 1983; Van De Meene et al., 2006). Also, it was shown that polyphosphate exists in two different fractions inside the cytoplasm, one bound to magnesium ions, while the other isn't. The role of polyphosphate in storage of metals was as well confirmed in cyanobacteria on organism *Plectonema boryanum* (Baxter & Jensen, 1980).

It has been shown that *ppx* transcript levels and as well the abundance of PPK and its activity were elevated under phosphate starvation in agreement with an idea that polyphosphate serves as cell's reserve of inorganic phosphorus. (Gómez-García et al., 2003). Furthermore, impaired growth of *ppx* mutant under normal cultivation conditions was recorded. The same study identified PPX protein as the only enzyme with exopolyphosphatase activity in this species. Microscopic studies on *Synechocystis* PCC 6803 using DAPI to visualize polyphosphate granules inside the cells showed how its abundance depends on phosphate levels in the medium. Further, cells are able to synthesise huge amount of polyphosphate in just a couple of minutes after addition of phosphate to phosphate-starved cultures (Voronkov & Sinetova, 2019).

Heterogeneity in the amount of polyphosphate among different cells was observed with around 30% of the cells having polyphosphate granules in conditions of exponential growth.

Gene *phoU* has also been studied in *Synechocystis* where it was shown that deletion of *phoU* leads to higher phosphate uptake and higher levels of polyphosphate (Morohoshi et al., 2002). Expression of genes under *pho* regulon control has also been investigated in another non-diazotrophic cyanobacteria *Synechococcus elongatus*. Their expression was multifold higher in phosphate-free medium. (Pitt et al., 2010).

Further, phosphate-starved cells of *S. elongatus* can accumulate as much as 60% of total cell phosphorus as polyphosphate once phosphate has been reintroduced, while in vegetative growth polyphosphate makes just 10% of total phosphorus pool. Also, activity of polyphosphate-synthesizing enzymes is around 30-fold higher under those conditions (Grillot & Gibson, 1979). This polyphosphate-overaccumulating ability is a part of *phosphate-luxury uptake* strategy common among organisms from phosphate-poor environments where phosphate is often the limiting nutrient for growth (Solovchenko et al., 2020).

Studying dynamics of polyphosphate granules degradation and DNA synthesis in *S. elongatus* showed colocalization of the two polymers and how DNA synthesis is followed by the process of polyphosphate degradation (Seki et al., 2014).

In *Synechocystis* an existence of PPK1 (sll0290) and of type 2 PPK2 (slr1363) with polyP: AMP phosphotransferase activity can be inferred based on protein homology (annotation data from: https://www.genome.jp/dbget-bin/www_bget?gn:T00004).

1.5. Bacterial dormancy as a survival strategy

Prokaryotic organisms possess an ability to enter dormancy upon transfer to adverse environmental conditions. This state is a long-term survival strategy characterised by virtually no metabolic activity and as such requires highly regulated process of entering dormancy by gradually shutting-down primary energy metabolism and genome's transcription levels (Rittershaus et al., 2013). After the first phase of cell's shutdown starts an accumulation of various storage polymers and proteins involved in the maintenance of a dormant state and also of those necessary for the trigger of the gradual reconstitution of its primary metabolism once the environmental conditions become favourable (Klotz & Forchhammer, 2017; Rittershaus et al., 2013). Bacterial ability to survive stressful conditions is crucial for their spread to new locations and is of human health interest in terms of bacterial drug resistance.

1.6. *Synechocystis* PCC 6803 as a model organism for the study of nitrogen-induced chlorosis

Cyanobacterium *Synechocystis* PCC 6803 (hereafter *Synechocystis*) serves as a model for studies of photosynthetic non-diazotrophic microorganisms. Its fully sequenced genome (3.57 million base pairs) consist of around 4,500 genes with more than 46% of unannotated genes (Fujisawa et al., 2017) As such is considered as an example of a genome-streamlined prokaryotic photosynthetic organism. It is naturally competent and easy to cultivate which makes it a perfect model for the studies of photosynthesis and has a prospective bioengineering role as a producer of various biological compounds of economic interest using a few simple input molecules (Yu et al., 2013).

Synechocystis is an autotrophic organism that performs oxygen-producing photosynthesis with certain differences in comparison to plants in terms of existence of a cyanobacterial-specific light-harvesting complex called phycobilisomes. As well, it possess a carboxysome compartment responsible for increasing local carbon dioxide concentration leading to enhanced carbon fixation by the Ribulose-1,5-bisphosphate carboxylase-oxygenase (RuBisCo).

As a non-diazotrophic organism it is unable to fixate atmospheric nitrogen unlike some other species of cyanobacteria such as order *Nostocales*. Nitrogen from the surrounding is transported into the cell in the form of nitrate and is reduced to ammonium by the activity of nitrate and nitrite reductase followed by its conversion into glutamine through the activity of GS-GOGAT (glutamin synthetase/glutamin oxoglutarate aminotransferase) pathway (Forchhammer & Schwarz, 2018). The ability of *Synechocystis* to adapt to nitrogen starvation is a widely studied phenomena of bacterial survival mechanism. The rapid acclimation to the lack of nitrogen by profoundly modifying its metabolism and rearranging of photosynthetic machinery has been characterized in detail. It serves as a well-investigated example of bacterial survival strategy with the data on changes on both proteome, phosphoproteome (Spät et al., 2018) and transcriptome (Choi et al., 2016) level and, as well, on physiological adaptations (Doello et al., 2018) associated with the transition to a dormant state.

The shift to nitrogen-free medium stimulates a series of metabolic changes induced by the accumulation of 2-oxoglutarate as a consequence of lack of glutamine synthesised from ammonia and glutamate. Accumulated 2-oxoglutarate serves as an indicator of elevated carbon/nitrogen ratio which leads to activation of PII protein as well as NtcA transcriptional factor involved in transcriptional changes associated with the adaptation to nitrogen starvation

(Klotz et al., 2015). The adaptations include increasing the activity of glutamine-synthase through synthesis of small regulatory peptides. Then, PII protein – a well-studied sensor of both cell's energy status and carbon to nitrogen ratio activates series of processes including synthesis of glycogen to balance cell's carbon to nitrogen ratio (**Figure 1**).

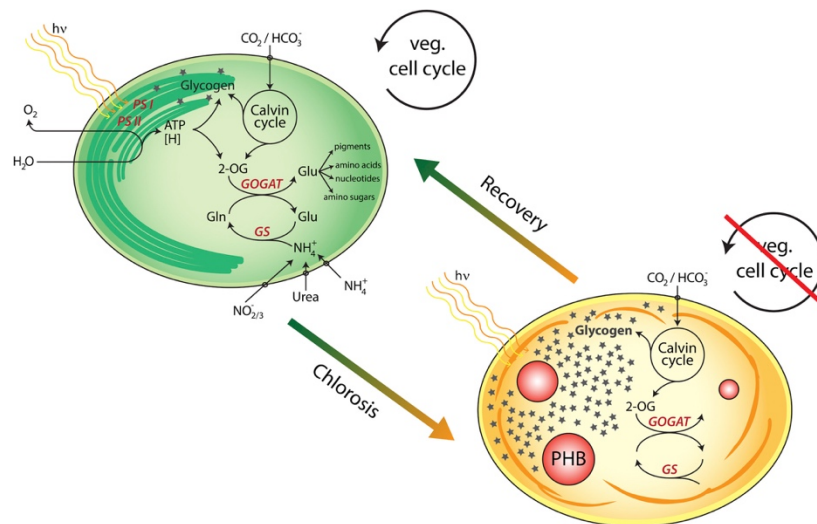


Figure 1. - Model of metabolic and morphological changes during chlorosis caused by nitrogen starvation in *Synechocystis*. (Klotz et al., 2016).

Lack of nitrogen leads to down-regulation of energy-requiring processes involved in synthesis of nitrogen-containing compounds such as nucleotides and amino acids. Consequently, reduced demand for energy in the form of ATP and necessity for redistribution of nitrogen-containing compounds causes degradation of proteins including phycobilisomes and of light harvesting complex. This can be seen as bleaching of cyanobacterial culture observable around one day after the shift to nitrogen-deplete media. During this period cells perform one more cell division and thereupon their decreased energetical demand is sustained with the residual photosynthetic activity (Forchhammer & Schwarz, 2018).

Glycogen is not synthesized in exponentially growing cells during conditions of constant light. It starts accumulating at the beginning of nitrogen-induced chlorosis and its levels reach a maximum value around seventh day of chlorosis after which it starts slowly degrading. Glycogen degradation was shown to have a crucial role in fuelling the process of resuscitation from nitrogen-induced chlorosis. The enzymes involved in its degradation such as glycogen phosphorylase (glgP) and Glucose-6-P dehydrogenase (ZWF) are accumulated during nitrogen starvation in order to fuel fast reawakening of the cells from dormancy once nitrogen is again available (Doello et al., 2018; Koch et al., 2019). Consequently, a mutant lacking glgP2, the first enzyme in the process of glycogen catabolism is unable to degrade glycogen and perform

transition from nitrogen starvation to vegetative growth. The main control of glycogen degradation is achieved through the phosphorylation state of the phosphoglucosyltransferase (PGM) protein (Doello et al., 2018). Process of resuscitation from nitrogen starvation starts as early as 20 minutes after the reintroduction of nitrate to the media, characterised by a fast ATP increase whose levels thereafter remain constant during the course of resuscitation. In the following hours, glycogen degradation supports respiration which provides energy for the reorganisation of the cell's structure for the first 24 hours of resuscitation, enabling cells to finally switch again to autotrophic metabolism (Doello et al., 2018). These changes can be observed in both transcript and protein abundance for genes and proteins involved in translational machinery including ribosomal proteins and translational factors. As well, it includes energy-related processes with genes and proteins for ATP synthase, RuBiSco and carboxysome (Spät et al., 2018). After 16 hours starts the production of photosynthetic pigments and the reassembly of thylakoid membranes (**Figure 2**) during which cell's energy supply depends both on photosynthesis and respiration. Between 24 and 48 hours after the start of resuscitation, cell's autotrophic metabolism starts taking over the main energy supply. The regreening of the cyanobacterial culture can be clearly seen, after which follows a cell division and a reconstitution of normal vegetative growth.

Another storage polymer accumulated in chlorosis is polyhydroxybutyrate whose degradation starts in late resuscitation after autotrophic metabolism had already been reconstituted. Mutants in PHB-synthesizing enzymes demonstrate almost normal resuscitation which leads to conclusion that PHB doesn't have an important role in this process (Koch et al., 2019).

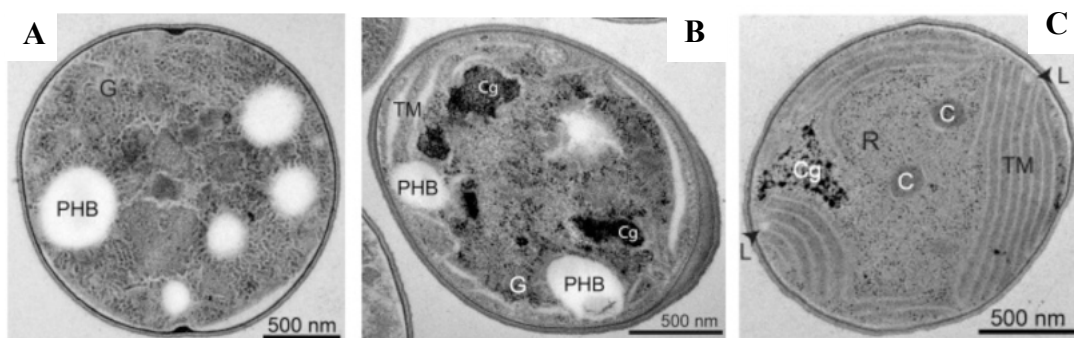


Figure 2 - Morphology of *Synechocystis* cell during nitrogen-induced chlorosis and resuscitation visualised by transmission electron microscopy. **A**) 1-month old nitrogen-starved cell, **B**) 24 hours after resuscitation from nitrogen starvation, **C**) exponential growth. G, glycogen granules; PHB, polyhydroxybutyrate granules; Cg, cyanophycin granules; C, carboxysomes; TM, thylakoid membranes; R, ribosomes; L, lipid bodies. Adapted from Klotz et al. (2016).

2. THE AIM OF THESIS

While synthesis and utilisation of polymers such as glycogen, cyanophycin, and PHB has been extensively studied under nitrogen starvation and other stressful conditions in *Synechocystis* (Damrow et al., 2016; Koch et al., 2019), the role of polyphosphate during stress acclimation in this microorganism remains uninvestigated. Current knowledge on polyphosphate in *Synechocystis* and other cyanobacteria is mainly based on a few microscopic studies and on quantification methods using DAPI to stain whole cell extracts – a method that doesn't provide absolute quantification of this polymer and is biased towards matrix composition. As well, knowing that *Synechocystis* - a model nonfilamentous cyanobacteria with huge biotechnological potential has a polymer whose role is poorly characterised has motivated this study to investigate it. Further, possible application of studies on regulation of polyphosphate metabolism could help in development of strains capable of bioaccumulation of inorganic phosphate from wastewater in a process of bioremediation.

This master thesis aims to elucidate the role of polyphosphate in *Synechocystis* by a) determination of absolute amount of polyphosphate in *Synechocystis* using the so-called *gold standard* for absolute polyphosphate quantification (phenol-chloroform extraction/ethanol precipitation followed by degradation with purified PPX), b) studying a mutant unable to produce polyphosphate – the first such study in cyanobacteria – in order to determine its role under vegetative growth and nitrogen starvation, and c) characterising the first cyanobacterial polyphosphate kinase enzyme.

3. MATERIALS AND METHODS

3.1. Cultivation of cyanobacterial cultures

Liquid cultures of *Synechocystis* were grown in 50 ml of BG-11 medium (**Table S1**) under conditions of constant light of 30-40 $\mu\text{Em}^2\text{s}^{-1}$ with constant shaking (120 rpm) at 28 °C. Abundance of cells in liquid culture was estimated based on optical density at 750 nm (OD_{750}) where OD_{750} value of 1 corresponds to 10^8 cells in 1 ml of liquid culture.

Stock cultures of glucose-tolerant wild-type and glucose-tolerant *ppk* mutant were reinoculated to fresh BG-11 medium every 10-15 days, with 50 $\mu\text{g/ml}$ of spectinomycin added to the *ppk* cultures.

For chlorosis experiments, an exponentially growing culture ($\text{OD}_{750} = 0.5-0.8$) was spun-down (4,000 g, 10 min, RT) and washed two times with 25 ml of nitrogen-free BG-11 medium (BG-0) and was then inoculated to a final $\text{OD}_{750} = 0.4$ and was afterwards kept at 40-50 $\mu\text{Em}^2\text{s}^{-1}$. Resuscitation of nitrogen-starved cultures was induced by addition of either NaNO_3 or KNO_3 in equal amounts as in BG-11 media.

For phosphate-starvation experiments cells were washed two times with phosphate-free BG-11 medium (KCl added in equimolar amounts to prevent potassium-starvation) and subsequently diluted to $\text{OD}_{750} = 0.25-0.3$. Recovery from phosphate-starvation was induced by addition of K_2HPO_4 in the same concentration as in BG-11.

Three biological replicates were used in all experiments, unless otherwise specified.

3.2 Visualisation of polyphosphate in *Synechocystis* using DAPI

Polyphosphate granules inside cells of *Synechocystis* were visualised as already described for this organism (Voronkov & Sinetova, 2019). Briefly, 1 ml of cyanobacterial culture was spun-down by centrifugation at 10,000 g for 5 min at room temperature (Eppendorf 5804R). Cells were then fixed by incubation with 1 ml of freshly prepared 4% formaldehyde in phosphate-buffered saline (PBS; 137 mM NaCl, 2.7 mM KCl, 1.8 mM KH_2PO_4 , 10 mM Na_2HPO_4 ; pH 7.4) buffer for 15 min. Then, the cells were washed three times with 1 ml of PBS after which they were incubated in the dark for 30 min with 500 μl of 10 $\mu\text{g/ml}$ of DAPI solution (Sigma-Aldrich). Afterwards, the cells were washed three times using 1 ml of PBS buffer. Finally, they were kept in 500 μl of PBS at 4 °C for maximum of 3-4 days or directly

visualised under the fluorescent microscope (Leica DM5500B, objective Leica HCX PL FLUATAR (100x/1,30 PH3)). For this purpose, 10 µl of stained cell suspension was dropped on agarose-covered glass slides. For the DAPI-polyphosphate detection, a cyan-fluorescent protein filter was used (Zeiss Filter Set 47, excitation: BP 435/40 nm, emission: BP 485/40 nm). A DAPI-DNA signal was detected using DAPI filter (Zeiss Filter Set 02, excitation: G 365/40 nm, emission: LP 440/40 nm). Chlorophyll autofluorescence was visualised using Cy3 filter (Zeiss Filter Set 47, excitation: BP 554/40 nm, emission: BP 568/40 nm). Image acquisition was done by Leica DFC 360 FX camera and analysed with the help of ImageJ software (ImageJ). The percentage of cells with polyphosphate granules in exponentially growing, chlorotic and resuscitating cultures was estimated by counting the total number of cells and the number of cells with visible polyphosphate granules in three biological replicates of WT. At least 200 cells were counted per condition. Statistical significance of the proportion of polyphosphate-containing cells was assessed by a t-test.

3.3. Segregation check of *ppk*

Polyphosphate kinase mutant (constructed by Sofia Doello) with the spectinomycin insertion in the coding region of *sl10290* gene coding for PPK was checked for chromosome-segregation by colony PCR.

A single colony was picked from an agarose plate and put into a tube with 10 µl of PCR Master Mix. A PCR was performed with following reagents and conditions:

PCR Master Mix:

- 5 µl of 2x Red Taq Master Mix (Amplicon)
- 0.5 µl of primer fw1 *ppk* seg check (**Table S3**)
- 0.5 µl of primer rev *ppk* seg check
- 0.5 µl of primer rev2 *ppk* seg check
- 3.5 µl of sterile water

Colony PCR conditions (PCR Senqoquest):

Initial denaturation: 90 °C 30 s

Denaturation: 98 °C, 30 s	}	30x cycles
Annealing: 55 °C, 30 s		
Elongation: 72 °C, 180 s		

Final elongation: 72 °C, 5 min

Agarose gel (1%, 200 ml) was prepared in Tris-acetate-EDTA (TAE; 40 mM Tris, 20 mM acetic acid, 1 mM EDTA, pH 8.0) buffer with 7 µl of gel stain Midori Green Advance (Nippongenetics). 10 µl of each PCR product and 4 µl of GenLadder (Gennaxon) was added to the wells. The gel-electrophoresis was run at 130 V/cm for 20 min. The gels were visualized under UV light.

3.4. Quantification of polyphosphate in *Synechocystis*

A following protocol for extraction and quantification of polyphosphate was used (adapted for *Synechocystis* from Bru et al., 2017):

A sample of 6 ml of *Synechocystis* liquid culture was snap-frozen in liquid nitrogen for 5 s and was then centrifuged (Eppendorf 5804R, 13,000 g, 2 min, 4 °C) and washed with 2 ml of Tris-buffered saline (TBS; 50 mM Tris-HCl, 150 mM NaCl; pH 7.5). Cell pellets were frozen in liquid nitrogen and then kept at – 80 °C . Cell pellets were incubated with 100 µg/ml lysozyme (Sigma-Aldrich) in 500 µl of Tris-EDTA buffer (TE; 10 mM Tris-HCl, 0.1 mM EDTA; pH 8.0) at 37 °C for 15 min. Subsequently, 500 µl of 25:24:1 phenol-chloroform-isoamylalcohol (Roth) was added to cells along with glass beads (0.1 mm, Sigma-Aldrich) after which they were lysed in homogenizer (MP FastPrep 24 5G; 5x cycles of 30 s, 3 min breaks, speed 6 m/s, 4 °C). Aqueous and organic phase were separated by centrifugation (13,000 g, 2 min, 4 °C) after which the aqueous phase was transferred to a screw-cap tube and an equal volume of phenol-chloroform-isoamylalcohol solution was added. The sample was vortexed vigorously for 1 min. Aqueous phase was transferred to a clean tube and was treated with 60 U of DNase I (Sigma-Aldrich) and 1.5 U of RNase A (Sigma-Aldrich) for 1 hour at 37 °C. For polyphosphate precipitation samples were transferred to tubes with 1 ml of absolute ethanol and 40 µl of 3 M CH₃COONa and left over-night at -20 °C. Next day, they were centrifuged (13,000 g, 20 min, 4 °C). The resulting polyphosphate-containing pellets was washed with 500 µl of 70% of cold ethanol. Pellets were left to dry for 5 min and 1 ml of sterile water was added to dissolve it. For polyphosphate degradation, 40 µl of ScPPX buffer (Tris-HCl, 25 mM MgCl₂, 250 mM NH₄CH₃COO; pH 7.5) was added to 150 µl of each sample along with 1 µg of purified ScPPX (or without ScPPX in control) and incubated at 37 °C for 15 min. Then, 50 µl of sample and control were added in duplicates to a well-plate containing 150 µl of water. 30 µl of Phosphate

Determination Kit Reagents (Abcam) was added to each well. Released phosphate was quantified spectrophotometrically by measuring absorbance at 630 nm on a plate-reader (Tecan Spark). A phosphate standard curve was generated. To account for presence of inorganic phosphate in the sample, phosphate value in control (without ScPPX enzyme) was subtracted from the sample's phosphate values.

The concentration of released phosphate was normalised to OD₇₅₀ and finally expressed in terms of intracellular concentration of polyphosphate in Pi residues. Volume of a single cell was calculated by considering a cell as a perfect sphere of a radius of 1 µm.

3.5. Quantification of glycogen in *Synechocystis*

Glycogen was extracted and determined as previously described (Klotz et al., 2015). Briefly, a 2 ml sample was taken and the culture's OD₇₅₀ was measured. The cells were washed (Eppendorf 5804R, 10,000 g, 10 min, RT) once with sterile water. Pelleted cells were incubated with 400 µl of 30% KOH (w/v) at 95 °C for 2 h to cause their disruption. Glycogen precipitation was caused by overnight incubation with 1200 µl of 70% ethanol. The samples were then centrifuged (Eppendorf 5804R, 10,000 g, 10 min, 4 °C) to pellet the glycogen; glycogen pellet was washed with 70% and 100% ethanol with centrifugations in-between. The pellet was then dried in Speed-Vac at 60 °C for 20 min. Next, a 1 ml of 100 mM CH₃COONa (pH 4.5) and 35 U of amyloglucosidase (Sigma-Aldrich) was added for glycogen degradation at 60 °C for 2 h. For glycogen determination, a 200 µl of sample was added to 1 ml of σ-toluidine reagent (6% σ-toluidine in 100% acetic acid (v/v)) and incubated at 100 °C for 10 min. The sample was left on in ice for 3 min and its OD₆₃₅ was measured on a micro-plate reader (Tecan Spark). The amount of glycogen was calculated based on the glucose-standard curve and its amount normalised to OD₇₅₀.

3.6. Quantification of ATP and ADP levels in *Synechocystis*

Samples were directly taken in the cultivation room and immediately frozen in liquid nitrogen, afterwards kept at -80 °C. Cells were broken by three cycles of shaking at thermo-block (99 °C, 900 rpm, 5 min) followed by freezing in liquid nitrogen. Samples were afterwards centrifuged (Eppendorf 5804R, 21,000 g, 1 min, 4 °C). The amount of ATP in the samples was determined using ATP Bioluminescence Assay Kit CLS II (Roche). Supernatant (10 µl) or ATP standard was added to 50 µl of ATP Reagent and luminescence expressed as relative

luminescence units (RLU) was recorded on luminometer (Sirius Berthold). The amount of ATP was calculated by comparing samples' RLU to ATP standard values.

For the quantification of ADP, same extraction procedure was used. ADP Assay Kit (Sigma-Aldrich) was used for its quantification.

3.7. Quantification of polyhydroxybutirate in *Synechocystis*

Polyhydroxybutirate content was determined as previously described (Koch et al., 2019). A sample of 25 ml and 15 ml was taken for exponentially growing and chlorotic cultures, respectively. The samples were centrifuged (Eppendorf 5417R, 4,000 g, 10 min, RT). The pellet was dried in Speed-Vac (Christ) for 4 h at 60 °C and its dry weight was determined. Then, each sample was boiled in glass tubes in 1 ml of concentrated H₂SO₄ at 100 °C for 1 h to break the cells and convert PHB to crotonic acid. Then, a 100 µl of this solution was mixed with 0.014 M of H₂SO₄ and was centrifuged (10,000 g, 10 min, RT) to remove cell debris. Then, 500 µl of supernatant was added to 500 µl of 0.014 M of H₂SO₄ followed by another centrifugation. The supernatant was used for high-pressure liquid chromatography (HPLC) on a Nucleosil 100 °C 18 column (Agilent) (125 by 3 mm). As a liquid phase, 20 mM phosphate buffer (pH 2.5) was used. Commercially available crotonic acids was used as a standard with a conversion ratio of 0.893. The amount of crotonic acid was detected at 250 nm. The amount of PHB has been normalized to cells' dry weight (CDW).

3.8. Spot-agar assay

A sample of 1 ml of liquid culture of each of the replicates of WT and *ppk* was taken, centrifuged (Eppendorf 5804R 13,000 g, 2 min, RT) and its OD₇₅₀ was adjusted to a value of 1 (corresponding to 10⁸ cells) using the medium of same composition as in liquid culture. Serial decimal dilutions of each biological replicate were made with culture medium after which 5 µl of each dilution of each replicate was plated on a BG-11 agarose plate (**Table S2**) and kept under either constant light (30-40 µE m² s⁻¹) or under day-night conditions (12 h of light (30-40 µE m² s⁻¹), 12 h of dark) to compare growth efficiency of WT and *ppk* in different conditions.

3.9. Purification of PPX1 from *S. cerevisiae*

A single-colony of BL21 (DE3) bacterial expression strain with pHis_ScPPX plasmid expressing recombinant His-tagged PPX1 from *S. cerevisiae* (kindly provided by Celina Frank) was inoculated in 5 ml of lysogeny broth (LB) with added ampicillin (100 µg/ml) for overnight incubation (37 °C, 120 rpm). The next day the culture was transferred to 2 l of LB medium with ampicillin and was kept growing (37 °C, 120 rpm) until reaching an OD₆₃₀ of 0.6–0.8. Then, Isopropyl β-d-1-thiogalactopyranoside (IPTG) was added to a final concentration of 0.5 mM for induction of protein expression and the flask was kept at 20 °C. The next day, the culture was centrifuged (Avanti Centrifuge J-26XP, 4,000 g, 10 min, RT) to pellet the cells. A 40 ml of cold lysis buffer (150 mM Tris-HCl, 150 mM KCl, 10 mM imidazole, 1 mM EDTA, 1 mM DTT, 1 mM phenylmethylsulphonyl fluoride (PMSF), 1 mg DNase I, 1 mg lysozyme (Sigma-Aldrich)) was added to the pellet. Cells were then broken by sonicator (Branson Sonifier 250) by 4x4 min of sonication (duty cycle 40%) with 4 min breaks in-between. Cell debris was pelleted by centrifugation (18,000 g, 60 min, 4 °C) and the protein-containing supernatant was filtrated (45 µm pore size) before applying to the Ni-NTA column (His Trap HP). The column was first prewashed with miliQ water and 25 ml of lysis buffer, after which the supernatant was added to it (flow: 1 ml/min) to bind the His-tagged ScPPX. Afterwards, the column was washed with 20 ml of wash buffer 1 (150 mM Tris-HCl, 150 mM KCl, 20 mM imidazole,) and 20 ml of wash buffer 2 (with 50 mM imidazole). The His-tagged ScPPX was eluted (flow: 5 ml/min) by elution buffer (150 mM Tris-HCl, 150 mM KCl, 250mM imidazole) and elution 0.5 ml-fractions were collected and checked for protein presence by Bradford reagent (RotiQuant, Roth). To confirm the presence of ScPPX (45 kDa) in elution fractions, a sodium dodecyl sulphate–polyacrylamide gel electrophoresis (SDS-PAGE) was run. The gel was loaded with cell debris, supernatant and flow-through fractions (all previously 10x diluted) and washing and separate elution fractions. Loading dye (Gel Loading Dye 6x, Biolabs) was added to 10 µl of each fraction and was boiled at 100 °C for 5 min before loading the gel.

An overnight dialysis of PPX was performed in dialysis buffer (50% glycerol, 100 mM Tris-HCl, 100 mM NaCl, 1 mM DTT; pH 7.5) and PPX was afterwards stored in aliquots at -20 °C. The concentration of purified ScPPX was determined by Bradford assay using BSA (bovine serum albumin) as a standard.

3.10. Cloning of PPK1 from *Synechocystis*

PCR was used to amplify *ppk* gene from purified genomic DNA of *Synechocystis* using primers with overhangs corresponding to XhoI site of pET15b plasmid (**Table S3**). Following PCR conditions were used:

Q5 PCR Master Mix:

5 μ l of 5x Q5 Reaction Buffer (Biolabs)
0.5 μ l of 10 mM dNTP
0.5 μ l of primer *ppk* fw ol pET15b
0.5 μ l of primer *ppk* fw ol pET15b
0.25 μ l of Q5 polymerase (Biolabs)
5 μ l of 5x Enhancer (Biolabs)
1 μ l of genomic DNA (140 ng/ μ l)
10.5 μ l of sterile water

Q5 PCR conditions (PCR Senqoquest):

Initial denaturation: 90 °C, 30 s

Denaturation: 98 °C, 30 s

Annealing: 58 °C, 30 s

Elongation: 72 °C, 4 min

} 35x cycles

Final elongation: 72 °C, 5 min

Plasmid pET15b (1 μ g) was digested with 1 μ g of XhoI restriction enzyme (Thermo Scientific) in 20 μ l of XhoI Buffer (Thermo Scientific) at 37 °C for 15 h. Digested plasmid and PCR product of *ppk* gene were visualised on an agarose gel (same conditions as mentioned above) and purified from the gel using DNA Gel Extraction Kit (Monarch) following manufacturer's instructions and their DNA concentration was determined (NanoPhotometer N120). Then, *ppk* fragment was ligated with pET15b using Gibson assembly following manufacturer's instructions (**Figure S1**). Insert (17.7 ng) and vector (41.4 ng) were mixed in 1:1 ratio in a final volume of 5 μ l and 15 μ l of Gibson master mix (**Table S4**) was added to it. Assembly was performed at 50 °C for 1 hour. A cloning product (1 μ l) was used for transformation by electroporation of *E. coli* NEB10 β strain. The cells were plated on LB-agar plate with ampicillin (100 μ g/ml) and single colonies were checked for *ppk* insertion by Colony PCR (using primers *ppk* fw ol pET15b and *ppk* rev ol pET15b). Positive colonies were then sent for sequencing using pET-specific primers to confirm the presence of complete *ppk* gene. Then, each colony

with *ppk* gene was used to inoculate 10 ml of LB medium with ampicillin (100 µg/ml). An overnight culture was used to perform plasmid isolation using MiniPrep Kit (Monarch). Purified plasmid was used to transform *E. coli* LEMO expressing strain.

3.11. Purification of recombinant PPK1

The procedure for induction of PPK1 expression and its purification was performed similarly as for ScPPX with following modifications. A different lysis buffer was used (50 mM HEPES, 500 mM NaCl, 1 mM MgCl₂, 5 mM imidazole, 1 mM EDTA, 1 mM DTT, 1 mM PMSF, 1 mg DNase I, 1 mg lysozyme; pH 8.0). As well, only one washing buffer was used (50 mM HEPES, 500 mM NaCl, 20 mM imidazole, pH 8.0) and a different elution buffer (50 mM HEPES, 500 mM NaCl, 500 mM imidazole, pH 8.0). Protein-rich fractions were dialysed into dialysis buffer (15% glycerol, 150 mM Tris-HCl, 150 mM NaCl, 1 mM DTT, 1 mM MgCl₂; pH 7.5) and purified PPK1 was afterwards stored at 4 °C.

3.12. Determination of polyphosphate-synthesizing activity of PPK1

In order to characterise polyphosphate-synthesizing activity of purified PPK1 enzyme a pyruvate kinase-lactate dehydrogenase (PK-LDH) coupled assay was used, as described earlier (Lapina et al., 2018). ADP release resulting from phosphate incorporation into polyphosphate from ATP was measured, where released ADP was used by PK (Sigma-Aldrich) to produce pyruvate from phosphoenolpyruvate (PEP). Generated pyruvate was converted to lactate by LDH (Sigma-Aldrich) with concurrent NADH oxidation. Change in absorption at 340 nm was monitored using spectrophotometer (SPECORD 210 PLUS, Analytik Jena AG) during 15 min. Amount of oxidised NADH corresponds to the amount of ATP utilised for polyphosphate chain elongation.

The assays was performed at 30 °C in 1 ml of LDH-PK buffer (50 mM NaH₂PO₄/Na₂HPO₄ or 50 mM imidazole pH 7.5, 50 mM KCl, 20 mM MgCl₂, 0.4 mM NADH, 1 mM PEP, 10 mM ATP, 0.5 mM DTT, 11 U of LDH, 15 U of PK, 5 µg of PPK1) and the reaction was started by the addition of ATP. Velocity slopes of each reaction were used to calculate activity of PPK (U/mg – µmol of ATP converted per 1 µg of PPK1 in 1 min). NADH molar absorption coefficient is 6178 L mol⁻¹ cm⁻¹ at 340 nm.

Computation of Michaelis constant (K_m) and maximal velocity (V_m) values from PPK activity of three replicates under ranging ATP concentrations was done by GraphPad Prism software (version 9) using non-linear regression. As well, $K_{0.5}$ value and Hill's coefficient for PPK1 under different phosphate concentrations was calculated using nonlinear fit allosteric analysis in GraphPad Prism. Dependence of PPK1 on phosphate concentration was compared to another PPK enzyme, namely PPK2c from *Ralstonia eutropha* (kindly provided by Prof. Dr. Dieter Jendrossek) under same reactions conditions (with 0.2 μg of PPK2c used).

3.13. Determination of polyphosphate-degrading activity of PPK1

To check if PPK1 can also utilise polyphosphate to produce ATP from polyphosphate and ADP, hexokinase-glucose-6-phosphate-dehydrogenase (HK-G6PDH) assay was used, similarly as previously described (Savchenko et al., 2008). The assay was performed at 30 °C in 1 ml of HK-G6PDH buffer (50 mM imidazole pH 7.5, 50 mM KCl, 20 mM MgCl_2 , 1 mM NADP, 5 mM glucose, 10 mM ADP, 5 mM polyP, 3 U of HK, 3 U of G6PDH, 5 μg of PPK1). The rate of ATP production was determined by following the change in absorption at 340 nm during 5 min, as a consequence of NADPH production. Hexokinase would convert produced ATP and glucose into glucose-6-phosphate, which was then used for NADP reduction by G6PDH.

4. RESULTS

4.1. Visualization of polyphosphate granules in *ppk* mutant, exponentially growing cultures, chlorosis and resuscitation

In order to see whether cells' polyphosphate accumulation dynamics changes in nitrogen starvation and resuscitation in comparison to exponential growth (EG), fraction of cells with polyphosphate granules visible after DAPI staining was determined. As well, absence of polyphosphate granules in *ppk* mutant was confirmed.

No polyphosphate granules were detected in *ppk* mutant after staining with DAPI (10 $\mu\text{g/ml}$) (**Figure 3**), while in WT around 50% of exponentially growing cells had polyphosphate granules (**Figure 4**). Proportion of cells with polyphosphate decreased to 40% (p-value = 0.03), and to 20% (p-value = 0.0003), in nitrogen-starved cells (10 d of nitrogen starvation) and resuscitating cells (24 h after resuscitation), respectively (**Figure 5**).

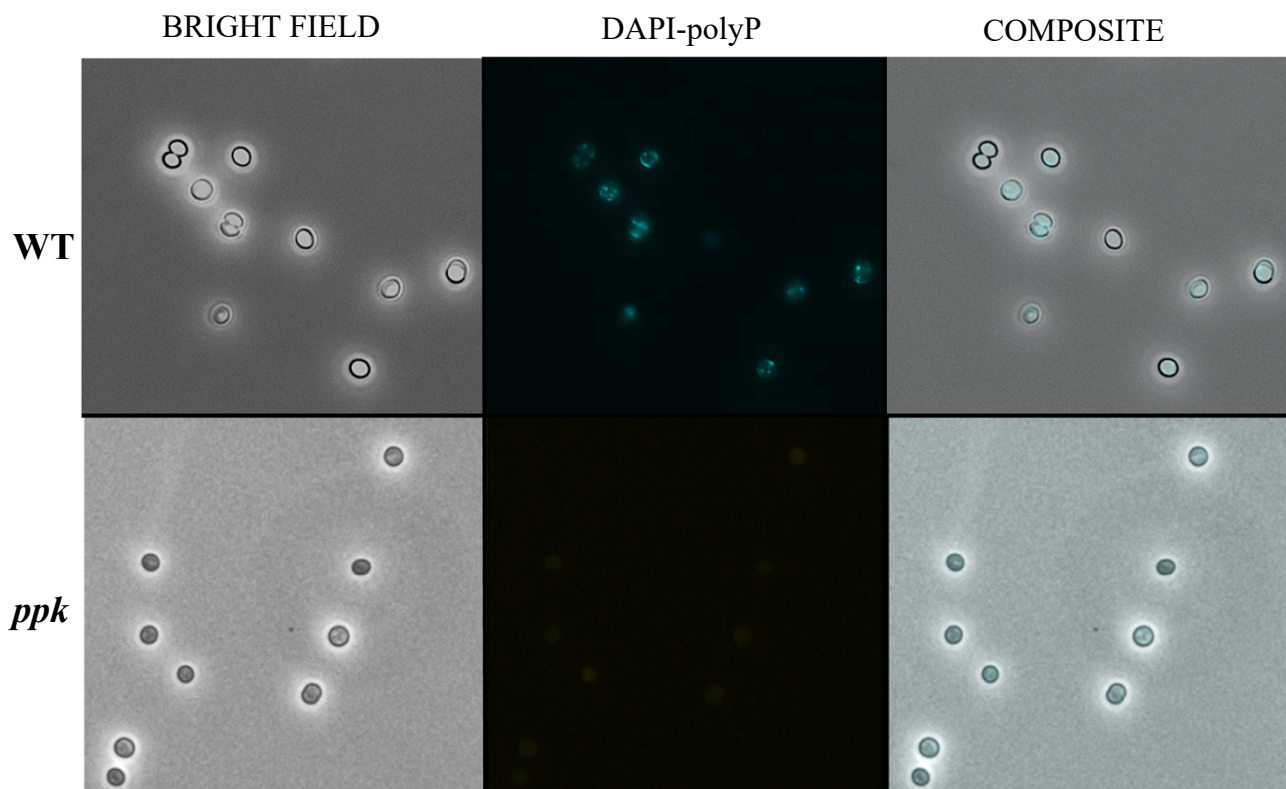


Figure 3 - Visualisation of polyphosphate granules stained with DAPI (10 $\mu\text{g/ml}$) in *Synechocystis* exponentially growing cells in a) WT and b) *ppk* mutant. First column represents bright field channel, middle column represents DAPI-polyP channel, and the last column is overlay of first two columns.

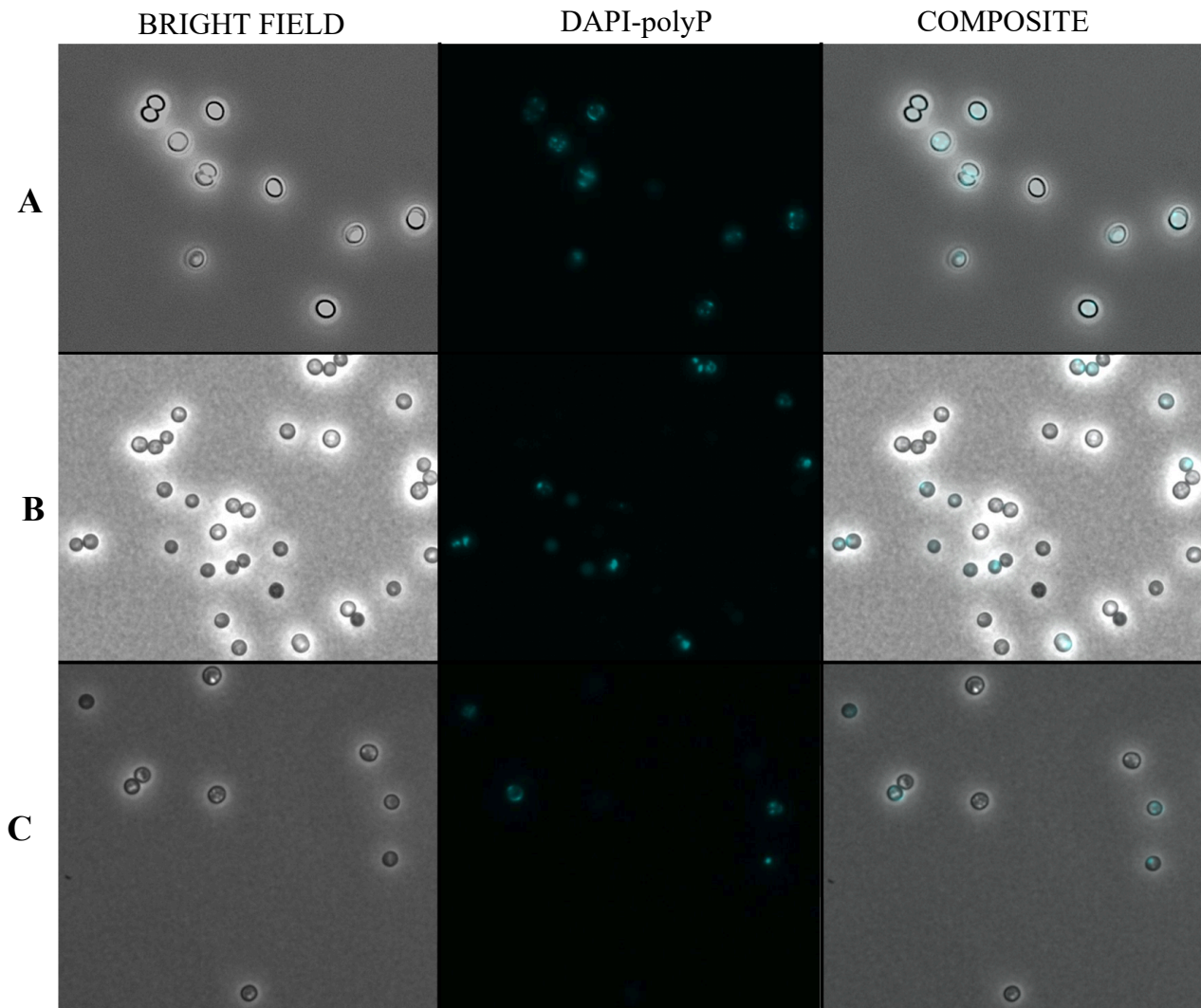


Figure 4 - . Polyphosphate granules in **A)** exponentially growing, **B)** 10 days chlorotic and **C)** 24 h +N resuscitating cells visualised by DAPI-staining.

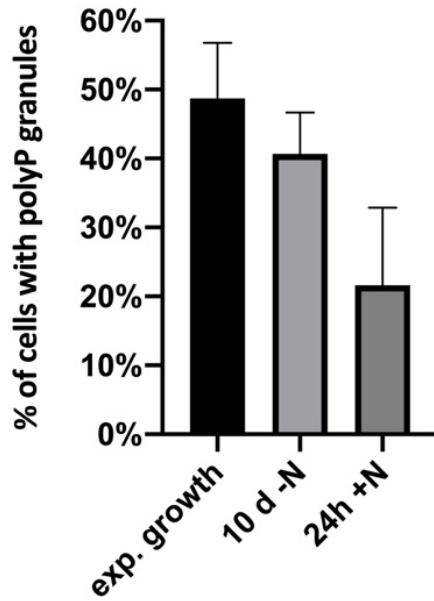


Figure 5 - Proportion of cells having polyphosphate granules visible under the microscope after DAPI staining in exponential growth, 10 d chlorotic cultures and 24 h after resuscitation. Error bars represent standard deviation (SD) of three biological replicates.

4.2. Spot-agar assay of *ppk* and WT cultures

Ability to recover from nitrogen-induced chlorosis in *ppk* was assessed by plating nitrogen-starved liquid cultures of WT and *ppk* on BG-11 (+N) agarose plates.

While *ppk* mutant shows normal growth under vegetative growth conditions (**Figure 6**) it demonstrates severely impaired resuscitation from nitrogen-induced starvation (**Figure 7**). Further, older nitrogen-starved cultures show more impaired resuscitation.

As well, after having had worked with *ppk* mutant for three months, it was observed that *ppk* developed adaptation enabling normal recovery from nitrogen starvation (**Figure 8B**). To find out whether this adaptation was due to developing an ability to synthesise polyphosphate, adapted *ppk* mutant's cells were stained with DAPI (**Figure 8C**). Nevertheless, adapted *ppk* doesn't produce polyphosphate granules visible under the microscope on DAPI-polyP channel.

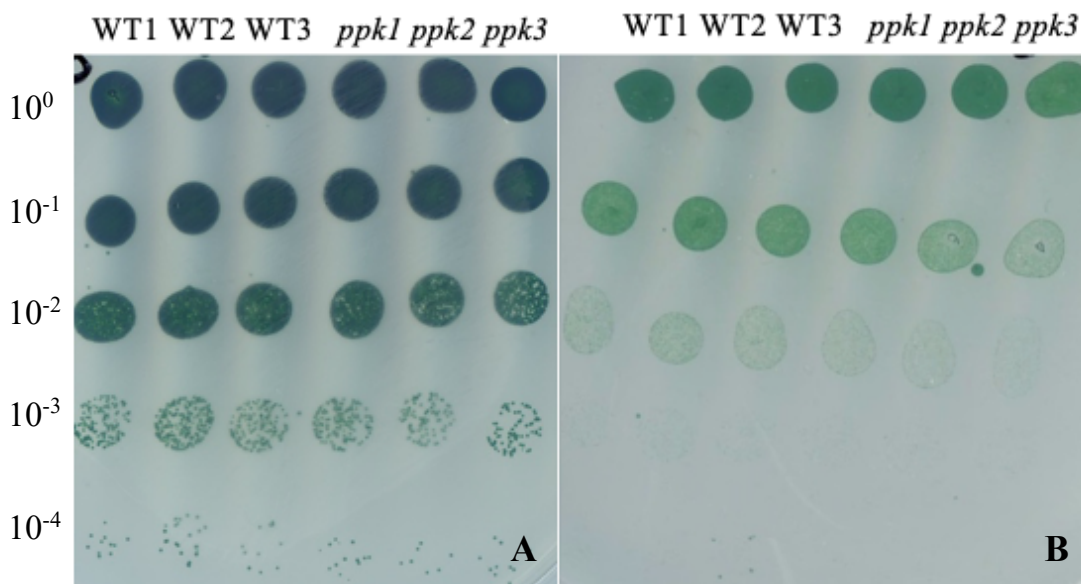


Figure 6 - Spot agar assay of WT and *ppk* under exponential growth on BG-11 agarose plates. **A)** constant light conditions ($30-40 \mu\text{E m}^2\text{s}^{-1}$), **B)** day/night conditions (12 h light of $30-40 \mu\text{E m}^2\text{s}^{-1}$, 12 h dark). Scale on the left represents serial dilutions of $\text{OD} = 1$ culture.

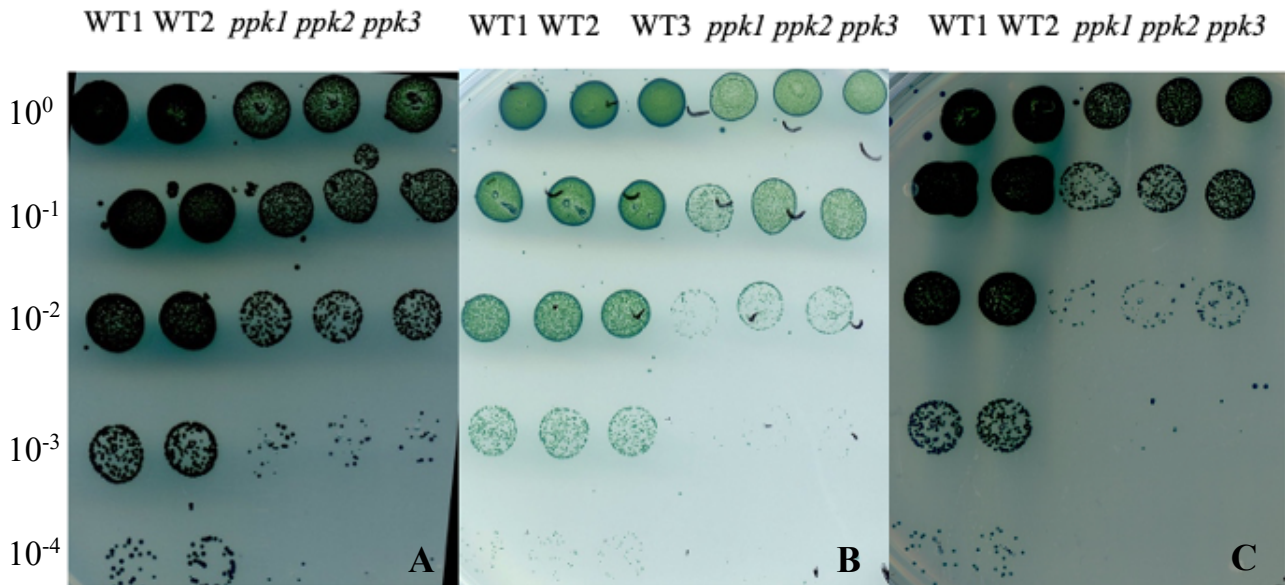


Figure 7 - Spot-agar assay of nitrogen-starved cultures of WT and *ppk* mutant plated on BG-11 (with nitrogen) agarose plates. *ppk* mutant shows impaired resuscitation from nitrogen chlorosis **A)** one week old nitrogen-starved cultures, **B)** two weeks nitrogen-starved cultures, **C)** three weeks nitrogen-starved chlorotic cultures. Scale on the left represents serial dilutions of OD = 1 culture.

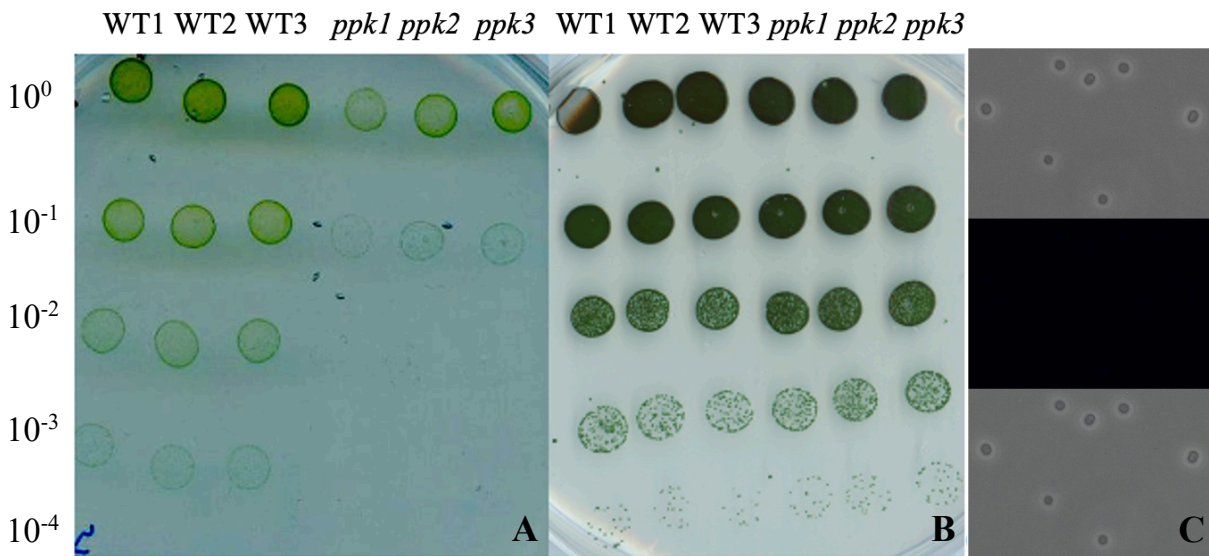


Figure 8 - **A)** Phosphate-starved cultures of WT and *ppk* plated on phosphate-free BG-11 agarose plates. **B)** Adapted *ppk* showing normal recovery from nitrogen chlorosis. Scale on the left represents serial dilutions of OD = 1 culture. **C)** DAPI staining of adapted *ppk* cells (from top to bottom: bright-field, DAPI-polyP channel and composite bright-field and DAPI-polyP channel)

4.3. Polyphosphate quantification in *Synechocystis*

Highly impaired nitrogen starvation recovery visible in drop-agar assay of *ppk* mutant suggested that polyphosphate may have an important role in resuscitation from nitrogen starvation. This further served as a motivation to investigate how polyphosphate level dynamics changes during nitrogen starvation and resuscitation from it. For this purpose, polyphosphate quantification assay based on phenol-chloroform extraction and ethanol precipitation followed by polyphosphate digestion by recombinant ScPPX was adapted for *Synechocystis*.

4.3.1. Optimization of protocol for polyphosphate quantification in *Synechocystis*

During optimization of polyphosphate extraction protocol, two extraction conditions were compared: two rounds of phenol-chloroform treatment versus only one round phenol-chloroform treatment (**Figure 9**). Two rounds of phenol-chloroform treatment gave higher yield of polyphosphate with smaller deviations between technical replicates. Therefore, from there on those conditions were used in the extraction of polyP. As well, in agreement with DAPI-visualisation experiments, no polyP was detected in *ppk* mutant.

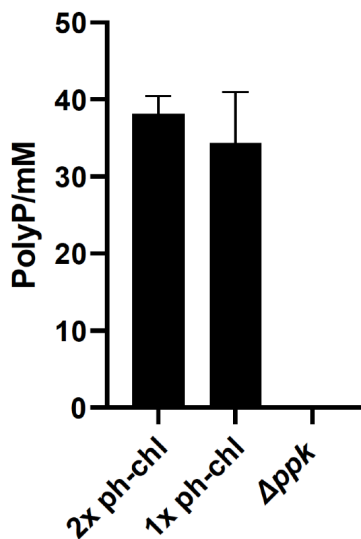


Figure 9 - Comparison of polyphosphate (**polyP**) content of the cells in exponential growth between two extraction conditions (one round of phenol-chloroform (**ph-chl**) treatment and two rounds of phenol-chloroform treatment). The amount of polyP is expressed as intracellular concentration of polyP in Pi-residues. Error bars represent standard deviation (SD) of three biological replicates.

The amount of polyphosphate determined by polyphosphate quantification protocol was compared to microscopic images of DAPI-stained polyphosphate granules to check protocol's

consistency with microscopic observations. For this purpose, polyphosphate was quantified in conditions for which it had been previously shown to have highly variant amounts of polyphosphate, specifically: a) 3 d of phosphate starvation, b) 1 h after reintroduction of phosphate to phosphate-starved cells, c) 24 h after reintroduction of phosphate to phosphate-starved cells and d) exponential growth.

The amount of polyphosphate determined by the protocol seems to be in-line with the microscopic observation of DAPI-stained polyphosphate granules (**Figure 10**). The amount of polyphosphate determined during exponential growth was around 51 mM. No polyphosphate could be detected after 3 d of phosphate starvation. Its amount increased drastically to 386 mM (7.5x of its EG value) 1 hour after reintroduction of phosphate to phosphate-starved cells. Polyphosphate content then decreased to 255 mM at 24 h after reintroduction of phosphate.

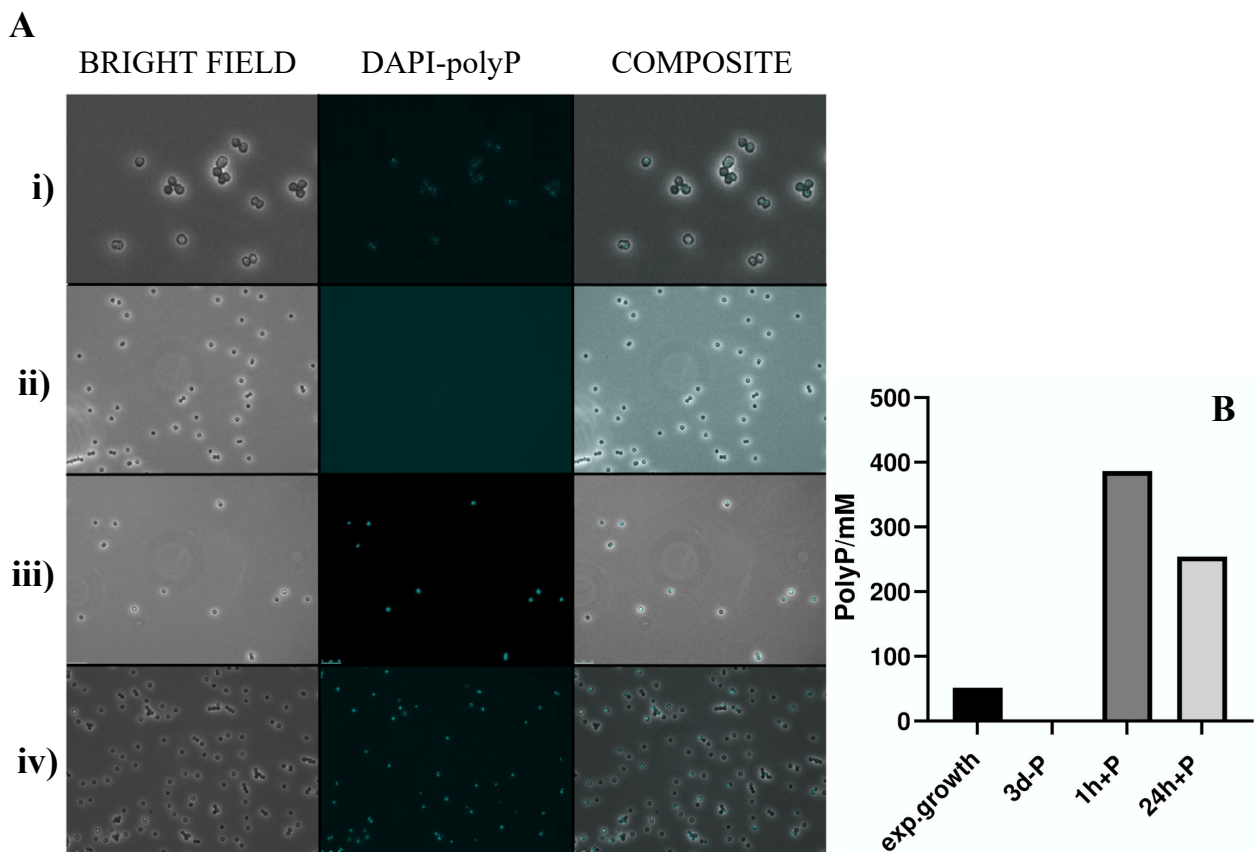


Figure 10 - Comparison of microscopic images of DAPI-stained polyphosphate granules inside *Synechocystis* cells with the results of polyphosphate quantification based on phenol-chloroform extraction and ethanol precipitation followed by degradation by ScPPX (exopolyphosphatase). **A**) DAPI-stained polyphosphate under following conditions i) exponential growth, ii) 3 d of phosphate starvation (**3 d -P**), iii) 1 h after reintroduction of phosphate (**1 h +P**) and iv) 24 h after reintroduction of phosphate (**24 h +P**). **B**) Intracellular concentration of polyphosphate (polyP) expressed in Pi-residues. Only one replicated was measured.

4.3.2. Polyphosphate levels during chlorosis and resuscitation

Amount of polyphosphate in the cells increased during nitrogen starvation (52 mM of polyP at 15 d of nitrogen starvation) compared to exponential growth conditions (25 mM of polyP, p-value = 0.0003). Surprisingly, no polyphosphate could be detected in the first day of nitrogen starvation. As well, the amount of polyphosphate decreased during resuscitation (42 mM of polyP at 24 h after addition of nitrogen, p-value = 0.045) (**Figure 11**).

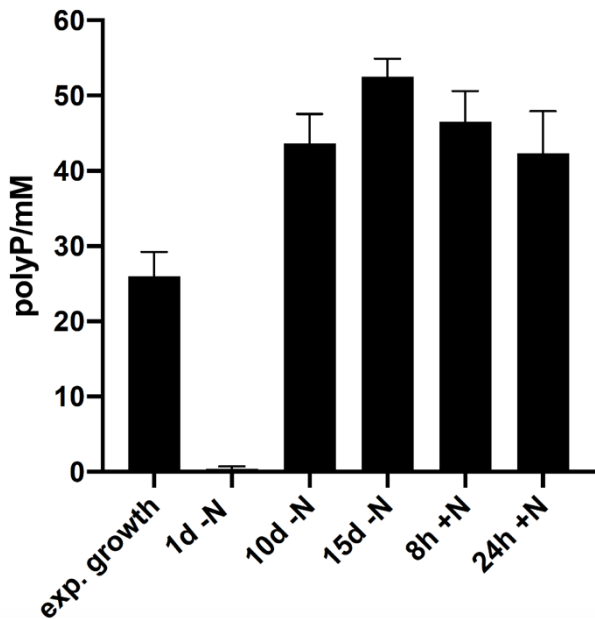


Figure 11 - Intracellular concentration of polyphosphate (polyP; expressed in Pi-residues) during nitrogen starvation (-N) and recovery from nitrogen starvation (+N). Error bars represent standard deviation (SD) of three biological replicates.

4.4. Comparison of glycogen synthesis and degradation in WT and *ppk* during chlorosis and resuscitation

Knowing that glycogen degradation is crucial for the process of recovery from nitrogen starvation, ability to synthesise and degrade glycogen was measured in *ppk* and WT cultures.

Wild type and *ppk* mutant show similar trend of glycogen synthesis during chlorosis. In recovery from nitrogen starvation, *ppk* mutant shows delayed glycogen degradation (**Figure 12**).

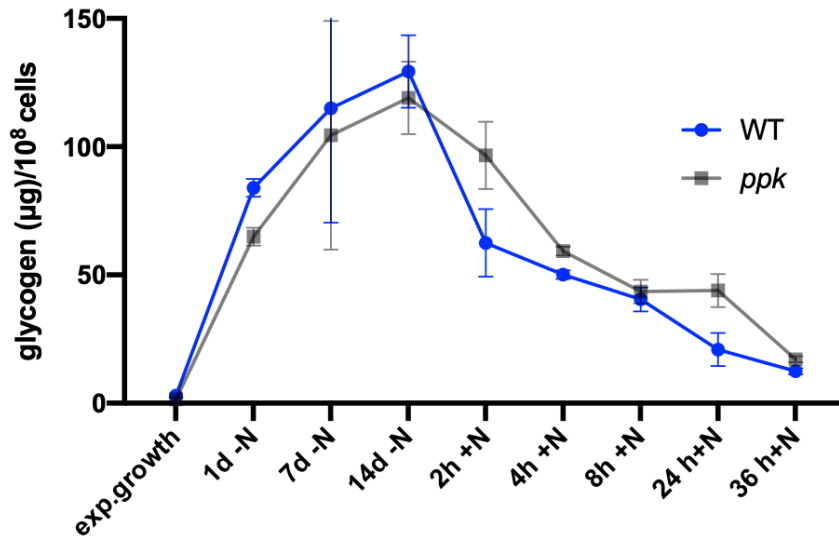


Figure 12 - Glycogen content of WT and *ppk* mutant in nitrogen-induced chlorosis (-N) and resuscitation (+N). Error bars represent standard deviation (SD) of three biological replicates.

4.5. ATP levels in resuscitation and upon entry in nitrogen-induced starvation

The next point of interest of this study was investigation of the lack of polyphosphate on the ATP levels in nitrogen starvation and recovery from it. Previous studies in other organisms often showed that *ppk* mutants have dysregulated ATP levels. As well, fast ATP changes normally occur both i) in entry in nitrogen starvation and ii) upon addition of nitrate to nitrogen-starved cultures. ATP levels of the *ppk* mutant were around 2.5x higher than in the WT in exponential growth conditions (p-value = 0.0002). More, *ppk* showed the same trend of ATP decrease following the shift to nitrogen-free medium (**Figure 13A**).

Further, similar was observed for *ppk* mutant following the addition of nitrate to BG-0 medium (**Figure 13B**), where a sharp ATP increase was observed both for the *ppk* mutant and the wild type 20 min after nitrate addition.

Then, it was also interesting to see whether ADP levels in the mutant were elevated too. The *ppk* mutant also had around 2x higher amount of ADP (p-value = 0.001) compared to WT during exponential growth (**Figure 14**).

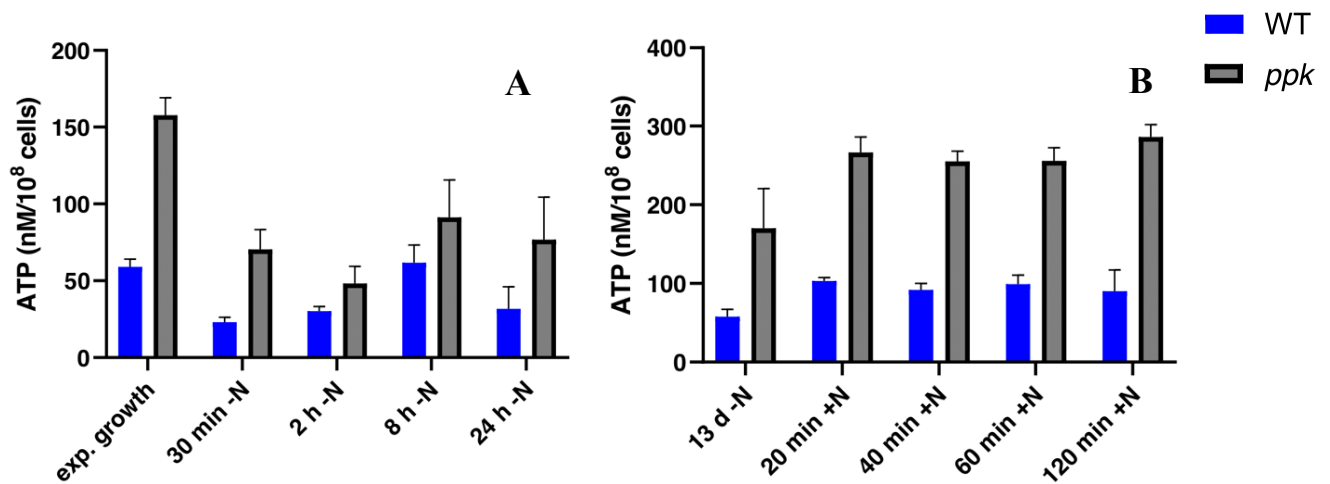


Figure 13 - ATP levels in WT and *ppk* after **A**) shift to nitrogen-free medium (+N) and **B**) after reintroduction of nitrate (+N) in the medium of two weeks old chlorotic cultures. Error bars represent standard deviation (SD) of three biological replicates.

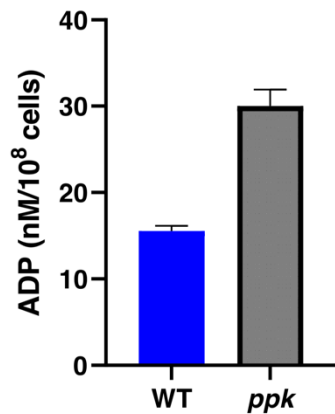


Figure 14 - Comparison of ADP levels between WT and *ppk* in exponential growth. Error bars represent standard deviation (SD) of three biological replicates.

ATP levels in adapted normal-resuscitating *ppk* mutant were also measured to see whether this adapted phenotype is due to restoring of normal ATP levels. The results show that adapted *ppk* mutant still has higher ATP levels in comparison to WT (**Figure 15**).

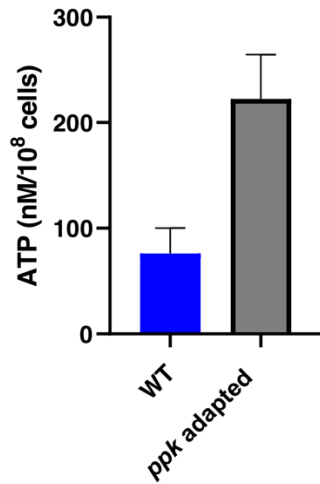


Figure 15 - Comparison of ATP levels at 14 days of nitrogen starvation in WT and adapted *ppk* mutant demonstrating normal resuscitating phenotype. Error bars represent standard deviation (SD) of three biological replicates.

4.6. PHB content of *ppk* and WT

Another polymer synthesized during nitrogen starvation is PHB.

No difference in the amount of PHB was measured between WT and *ppk* (**Figure 16**).

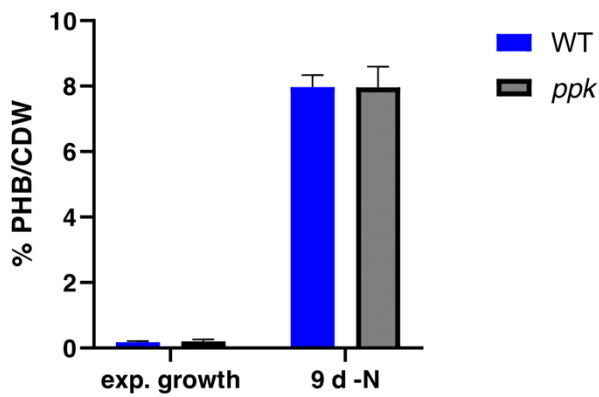


Figure 16 - Polyhydroxybutirate (PHB) content of WT and *ppk* in exponential growth and nitrogen starvation (9 d -N) expressed as a percentage of cell dry weight (CDW). Error bars represent standard deviation (SD) of three biological replicates.

4.7.1. Purification of PPK1 protein

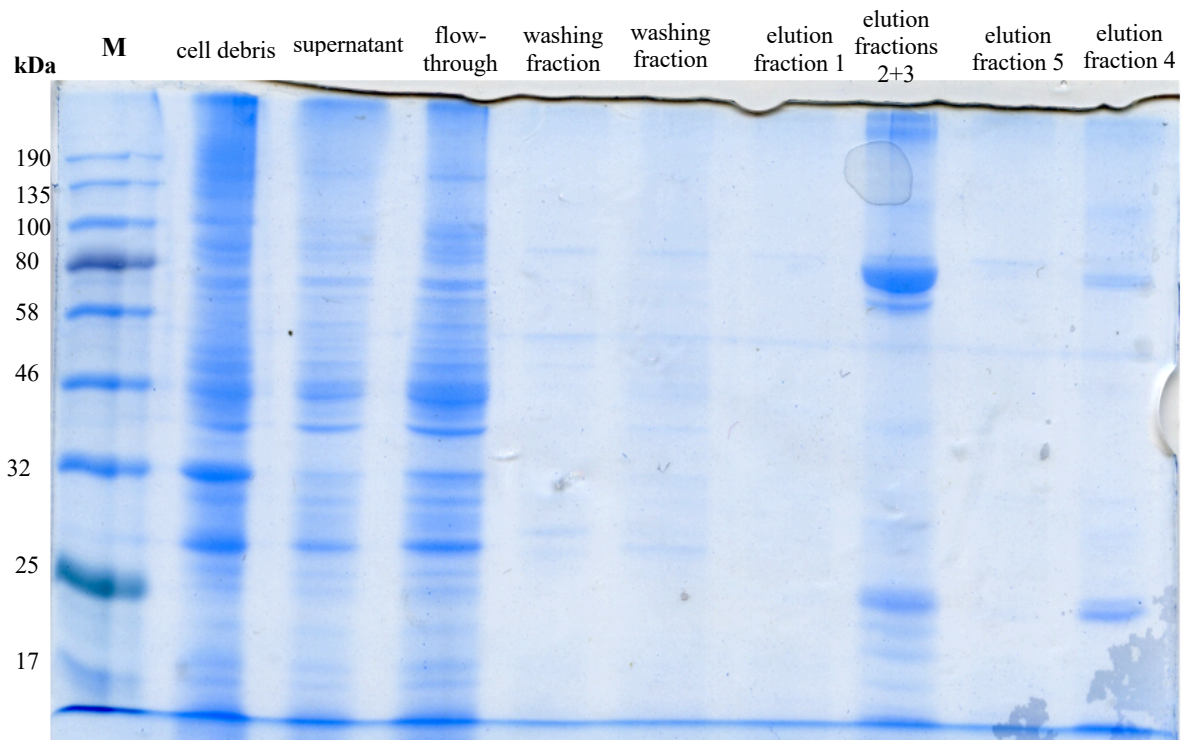


Figure 17 - SDS-PAGE electrophoresis of purification steps of His-tagged PPK1 overexpressed from *E. coli* LEMO strain using affinity Ni-NTA column. M - protein standard marker - 5 μ l (Color Prestained Protein Standard Broad Range, Biolabs). Amount of protein was 4 μ g for elution fraction 2+3. In other fractions, 10 μ l of each was added to the well (cell debris, supernatant and flow-through fractions were first 10x diluted) along 10 μ l of miliQ at 5 μ l of Gel Loading Dye (Biolabs). Proteins were stained and visualised by Coomassie blue (InstantBlue, Expedeon).

PPK1 from *Synechocystis* was over-expressed in *E. coli* LEMO strain by IPTG induction and then successfully purified by Ni-NTA affinity chromatography. It was eluted by elution buffer with 500 mM imidazole and was subsequently dialysed in Tris-HCl buffer with 15% glycerol (smaller amounts of glycerol caused its precipitation). It was afterwards stored at 4 $^{\circ}$ C for no longer than two weeks. A band in elution fractions close to a standard's band of 80 kDa corresponds to PPK1 (theoretical mass \sim 82.6 kDa) (**Figure 17**).

4.7.2. Polyphosphate-synthesizing activity of PPK1 from *Synechocystis*

Next, enzymatic assays were used to characterize reaction kinetics of PPK1 from *Synechocystis*. Polyphosphate-synthesizing activity was measured using PK-LDH coupled assay which detects ADP release.

PPK1 from *Synechocystis* shows high dependence on the presence of phosphate. It is completely inactive without phosphate and it experiences a sharp increase in polyphosphate-synthesizing activity as the concentration of phosphate increases from 20 mM to 40 mM (**Figure 18**). On the other hand, PPK2c from *R. eutropha* is fairly active without phosphate and it shows a three-fold increase in the activity upon addition of phosphate.

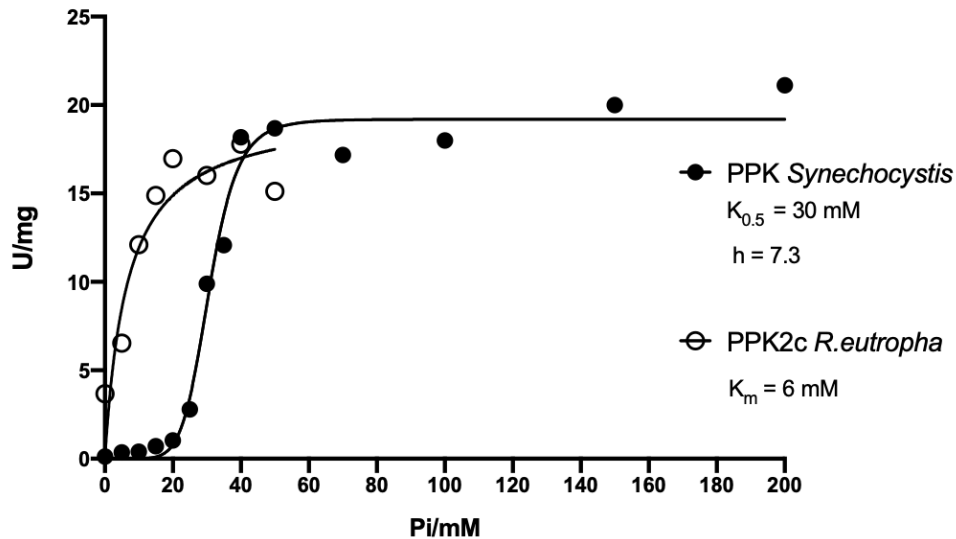


Figure 18 -Dependence of PPK activity on the presence of inorganic phosphorus (Pi). Black dots - **PPK1** from *Synechocystis*, white dots - **PPK2c** from *Ralstonia eutropha* (kindly provided by Prof. Dr. Dieter Jendrossek). The reaction was performed at 30 °C in PK-LDH buffer (with 50 mM imidazole) using ranging concentrations of $\text{NaH}_2\text{PO}_4/\text{Na}_2\text{HPO}_4$. The reaction was started by addition of 10 mM ATP. The assay was performed in 1 ml cuvette using 5 μg and 0.2 μg of PPK1 and PPK2c, respectively. Hill's coefficient (h) and $K_{0.5}$ were calculated using nonlinear fit in GraphPad Prism. Michaelis constant (K_m) of PPK2c was calculated by Michaelis-Menten kinetics analysis in GraphPad Prism. U/mg - μmol of ATP consumed per mg of PPK in 1 min.

In order to determine K_m value of PPK1, ranging concentrations of substrate (ATP) were used. K_m value of 1.35 mM of ATP and V_m of 17.4 U/mg were determined using Michaelis-Menten model in nonlinear regression analysis (**Figure 19**).

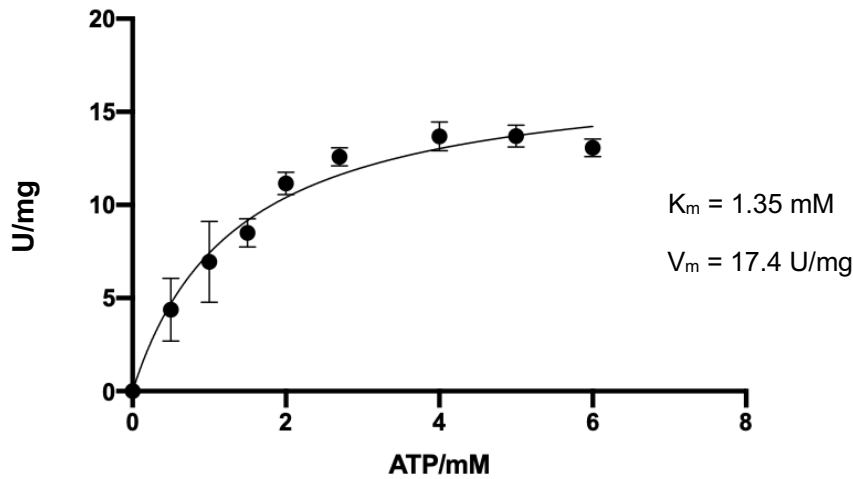


Figure 19 - Velocity dependence of PPK1 on concentration of ATP. Assay was performed at 30 °C in 1 ml of PK-LDH buffer (with 50 mM $\text{NaH}_2\text{PO}_4/\text{Na}_2\text{HPO}_4$) using 5 μg of PPK1. Reaction was started by addition of ATP. Michaelis constant (K_m) and maximal velocity (V_m) were calculated by Michaelis-Menten kinetics analysis in GraphPad Prism. U/mg - μmol of ATP consumed per mg of PPK in 1 min. Error bars represent standard deviation (SD) of three technical replicates.

Next point of interest was dependence of PPK1 activity on the presence of inorganic polyphosphate. Previous studies identified that PPK1 often requires polyphosphate as a primer in the reaction of polyphosphate chain elongation. For this purpose, 6 mM of polyphosphate (Sigma-Aldrich, chain length ~ 45 Pi residues) was added to PK-LDH buffer.

PPK1 shows no difference in activity between conditions with and without polyphosphate in the reaction buffer (p-value = 0.323) (**Figure 20**).

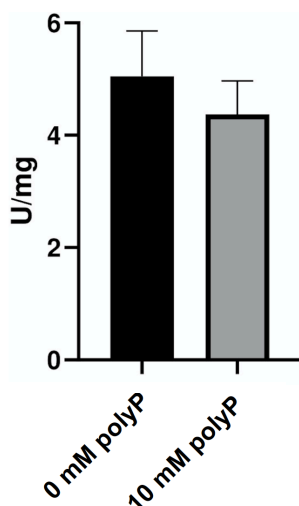


Figure 20 - PPK1 polyphosphate-synthesizing activity under conditions with (6 mM) or without polyphosphate (Sigma-Aldrich, chain length ~ 45 Pi residues). Assay was conducted in 50 mM of imidazole buffer with 10 mM of $\text{NaH}_2\text{PO}_4/\text{Na}_2\text{HPO}_4$ (Pi). U/mg - μmol of ATP

consumed per mg of PPK1 in 1 min. Error bars represent standard deviation of three technical replicates.

4.7.3. Polyphosphate-degrading activity of PPK1 from *Synechocystis*

As well, the opposite reactions of ATP generation by phosphate transfer from polyphosphate chain to ADP was studied by HK-G6PDH coupled assay using 5 mM of polyphosphate (Sigma-Aldrich, chain length ~ 45 Pi residues) and 10 mM of ADP as substrate. PPK1 polyphosphate-degrading activity isn't affected by the presence of inorganic phosphate, unlike its synthesizing activity (**Figure 21A**). Further, this reaction started reaching the plateau as soon as 5 min after its beginning (**Figure 21B**).

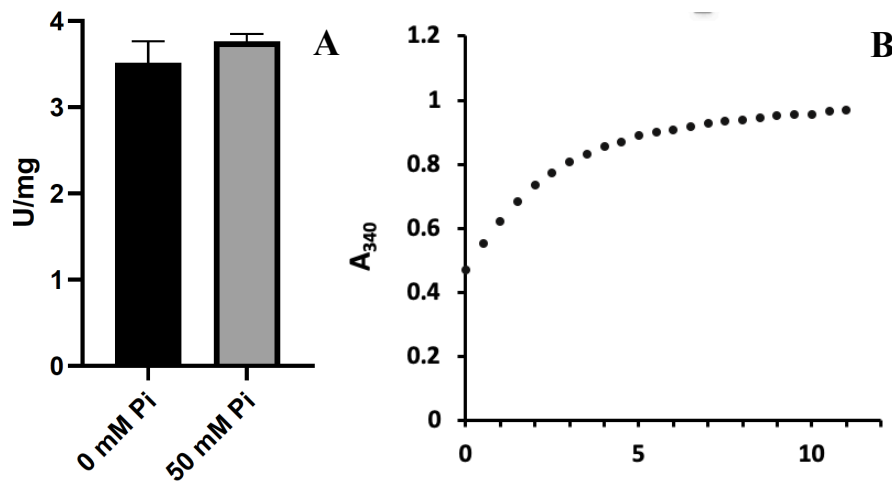


Figure 21 - Polyphosphate-degrading activity of PPK1 from *Synechocystis*. Assay was performed in 1 ml of HK-G6PDH buffer with 5 mM of polyphosphate (Sigma-Aldrich). Reaction was started by addition of 10 mM ADP. **A**) Dependence of polyphosphate-degrading activity of PPK1 under conditions with and without inorganic phosphate (Pi). Error bars represent standard deviation of three technical replicates. **B**) Increase in A₃₄₀ (absorbance at 340 nm) as a result of ATP production from ADP and polyphosphate.

5. DISCUSSION

Polyphosphate granules were successfully visualised by DAPI staining with around 50% of cells having visible granules (**Figure 5**), which is higher than the amount already reported for *Synechocystis* under normal growth (30%) (Voronkov & Sinetova, 2019). This result again confirmed that there exists heterogeneity among the cells in terms of polyphosphate accumulation strategy.

No polyphosphate granules could be seen in *ppk* mutant (**Figure 3**) confirming together with the results of polyphosphate quantification in *ppk* (**Figure 9**) that PPK1 is the only enzyme with polyphosphate-synthesizing ability in this organism. Next, the ratio of cells with polyphosphate granules seems to decrease to 40% during chlorosis and to 20% in resuscitation (**Figure 5**). This data isn't in line with the results of quantification of polyphosphate in chlorosis where total amount of polyphosphate increases two-fold during course of nitrogen-induced chlorosis (**Figure 11**). It could be that particular cells from the culture have different strategies in dealing with nitrogen starvation with some synthesizing more of polyphosphate and the others degrading it. Similarly, heterogeneity among different cells has too been reported for formation of PHB granules during nitrogen starvation (Koch et al., 2019).

Spot-agar assay used for testing recovery ability from nitrogen starvation showed that *ppk* mutant is highly impaired in resuscitation. Two-weeks old chlorotic cultures show around 100-fold impaired resuscitating ability (**Figure 7**). This initially suggested that polyphosphate could be of great importance in the process of nitrogen-starvation recovery. In contrast, *ppk* mutant grows normally under exponential growth conditions (**Figure 6**) suggesting that lack of polyphosphate doesn't have detrimental affect under normal conditions when cells are supplied with enough nutrients for growth. Interestingly, it has been already reported that *Synechocystis* mutant lacking PPX enzyme responsible for polyphosphate degradation is impaired in normal growth (Gómez-García et al., 2003) thereby suggesting that the cycling of polyphosphate, rather than polyphosphate *per se* is important in normal growth. Expectedly, *ppk* mutant exhibits impaired growth and faster bleaching of the culture in the phosphate-free media (**Figure 8A**).

Further, adapted *ppk* mutant with normal nitrogen starvation recovery phenotype (**Figure 8B**) still doesn't produce polyphosphate visible by DAPI staining (**Figure 8C**). This shows that polyphosphate probably isn't directly involved in the process of recovery from nitrogen starvation. This adapted mutant started showing normal-resuscitating phenotype after three

months of working on it (with the new stocks of the mutant being made every two weeks from the old one). It is therefore likely that the same selection pressure present in the stationary phase of culture is responsible for a mutation enabling normal resuscitation.

As well, *ppk* mutant tends to die faster during longer periods of chlorosis (~four weeks, data not shown), possibly because of lack of polyphosphate as a phosphate source in prolonged starvation.

Further, a question that raises is: if polyphosphate isn't present in all the cells in nitrogen chlorosis (**Figure 4**), how can it be that its absence affects so severely the recovery ability of *ppk* mutant? It could be that only a small amount of polyphosphate, not visible as granules inside the cells after DAPI-staining, is sufficient in the process of recovery. Alternative explanation is that maybe PPK1 enzyme itself, rather than polyphosphate is important during recovery.

Next, a protocol for absolute polyphosphate quantification based on phenol-chloroform extraction and ethanol precipitation followed by digestion by ScPPX was adapted for the first time in *Synechocystis*. Also, this is the first try of applying this protocol for absolute quantification of polyphosphate in some species of cyanobacteria. Previous attempts of polyphosphate quantification were mostly based on either DAPI staining of the whole-cell extracts (Martin & Van Mooy, 2013) or by tracing the amount of radioactively-labelled phosphate incorporated into acid-insoluble polyphosphate (Grillot & Gibson, 1979).

Intracellular concentration of polyphosphate of 26 ± 3.7 mM measured in exponential growth (**Figure 11**) corresponds to 3.3 ± 0.6 fg of phosphorus incorporated into polyphosphate per single cell. For comparison, recorded amount of polyphosphate in *S. elongatus* after reintroduction of phosphate was 8 fg/cell, while in *E. coli* it was around 0.8 fg/cell (Van Dien et al., 1997). More, a huge seven-fold increase in polyphosphate content was measured upon addition of phosphate to phosphate-starved cultures (**Figure 10**), in agreement with microscopic images and prior data on this organism (Voronkov & Sinetova, 2019). Further, polyphosphate quantification again confirmed that *ppk* mutant doesn't produce any polyphosphate (**Figure 9**). This adapted protocol can be used in the future for determination of polyphosphate in *Synechocystis* and other species of cyanobacteria.

This working protocol was then applied for polyphosphate quantification in nitrogen-induced chlorosis and resuscitation. Oppositely of expected, no polyphosphate could be detected at the first day of nitrogen starvation (**Figure 11**), probably due to an extraction artifact.

Polyphosphate granules are clearly visible under the microscope after DAPI staining at the first day of nitrogen starvation (data not shown). In order to determine polyphosphate content in the first day of nitrogen starvation, polyphosphate extraction procedure should maybe be repeated with a different cell-breakage protocol.

Cells seem to accumulate polyphosphate by two-fold during nitrogen starvation and consume around 20% of it in the first 24 hours of recovery from starvation (**Figure 11**). This increase in the amount of polyphosphate in chlorosis isn't in agreement with microscopic observations of polyphosphate granules. It may be that polyphosphate chains are of shorter length in nitrogen chlorosis, which could affect their visualisation with DAPI (Christ et al., 2020). The decrease in the amount polyphosphate during resuscitation is in agreement with microscopic data on the percentage of cells with polyphosphate granules. Therefore, it is likely to conclude that polyphosphate is degraded during the course of resuscitation.

Glycogen degradation ability, as the key process in the recovery from nitrogen starvation was tested as well, especially knowing that mutants unable to degrade glycogen have highly impaired recovery (Doello et al., 2018) - as is the case with this mutant. From these results it seems that *ppk* is unaffected in its glycogen synthesizing ability in nitrogen starvation. In contrast, it displays somewhat delayed glycogen degradation compared to the WT (**Figure 12**). One hypothesis was that polyphosphate may serve as a source of phosphate for glycogen phosphorylases in the process of glycogen degradation. This has likely been ruled out by the existence of polyphosphate-lacking mutant with normal recovery.

Then, control of ATP levels is important for nitrogen starvation (Doello et al., 2018) with cells being able to reduce ATP content to a half as early as 30 minutes after the shift to nitrogen-free medium. As well, the first step of recovery from nitrogen chlorosis is a rapid ATP increase upon addition of nitrate to the media. This served as a motivation to investigate if polyphosphate may be a source or a sink for ATP at the onset of nitrogen chlorosis and recovery from it, respectively. The results of ATP measurements show that *ppk* mutant has around two-fold higher ATP levels in both exponential growth and all stages of nitrogen starvation and resuscitation (**Figure 13**). It also experiences the same trend of ATP decrease and increase upon entry in chlorosis and recovery from it, respectively. Therefore, polyphosphate certainly doesn't serve as an ATP storage in adaptation to nitrogen starvation.

Elevated ATP concentration could perhaps inhibit glycogen degradation (Morgan & Parmeggiani, 1964), thereby indirectly affecting resuscitating ability of *ppk* mutant. Therefore, in this case, highly impaired resuscitating phenotype wouldn't be directly explained by the lack

of polyphosphate, rather perhaps by disrupted energy metabolism that prevents normal glycogen degradation. This assumption could be tested by studying glycogen-degradation ability of adapted *ppk* mutant.

As well, ADP content (**Figure 14**) is also around two-fold higher in *ppk* mutant, showing that it's not only ATP that is disrupted in *ppk*, but the whole adenylate pool with the ATP/ADP ratio remaining unaffected. Disrupted adenylate pool could possibly indirectly affect levels of cyclic di-AMP - which is an important signalling molecule with the role in stress adaptation in cyanobacteria (Agostoni et al., 2018; Rubin et al., 2018). Therefore, impaired nitrogen-chlorosis survival could perhaps be explained by disrupted ci-di-AMP signalling in *ppk* mutant - an indirect effect of dysregulated adenylate levels. Interestingly, it has been shown that polyphosphate itself is in fact a negative regulator of cAMP production through inhibitory binding to adenylate cyclase in *Mycobacterium bovis* (Guo et al., 2009).

It would be interesting to see if the levels of other phosphonucleotides are affected, too. Also, adapted *ppk* still has two-fold higher ATP (**Figure 15**), thus suggesting that the mutation enabling normal resuscitation isn't affecting ATP levels of adapted mutant.

As well, determination of adenonucleotides levels should be repeated with another method, such as HPLC to confirm that these results aren't due to method bias.

Higher ATP levels have been observed in PPK-deficient mutants in other organisms (McMeechan et al., 2007). In *Synechocystis*, elevated levels of ATP and adenylate pool was seen in mutants unable to produce glycogen as a consequence of dysregulated energy metabolism (Cano et al., 2018). Therefore, synthesis of polyphosphate may also be involved in energy homeostasis in *Synechocystis*.

In order to clarify what is the exact role of polyphosphate in nitrogen-starvation, a whole-genome sequencing (WGS) of adapted and non-adapted *ppk* mutant would be the most insightful way to tackle this question. WGS would help to find the exact mutation enabling normal recovery of adapted *ppk* mutant. This could pinpoint to a specific signalling pathway whose disruption harshly affects survival in nitrogen-induced chlorosis.

This is the first time that polyphosphate kinase has been purified and characterised in cyanobacteria. PPK1 from *Synechocystis* has an K_m value around 1.3 mM of ATP (**Figure 19**), which is similar to previously characterised PPK enzymes from other organisms (Ahn & Kornberg, 1990). As well, it has maximum activity of 17.4 U, while *E. coli* PPK has V_m of 51.1 U (Kumble et al., 1996). Further, it has a k_{cat} value of 23 s^{-1} . In contrast to most previously

reported PPK enzymes, PPK1 from *Synechocystis* shows a highly cooperative allosteric dependence on the presence of inorganic phosphate, with a Hill coefficient of 7.3 and a half-maximal activating concentration of 30 mM. The PPK1 enzyme studied here is completely inactive without phosphate and its activity sharply increases as concentration of Pi increases from 20 to 40 mM (**Figure 18**). Such an extreme cooperative allosteric regulation of PPK was never reported before. The only known sigmoidal allosteric regulated PPK was described from *Neisseria meningitidis* (Tinsley et al., 1993), where half maximal activation was achieved already with 1 mM phosphate. The sigmoidal curve of PPK1 activity of *Synechocystis* pinpoints to a cooperative type of binding of phosphate to at least seven allosteric sites. This observation can explain why cyanobacterial cells can rapidly accumulate polyphosphate as early as five minutes after reintroduction of phosphate to phosphate-starved cells (Grillot & Gibson, 1979; Voronkov & Sinetova, 2019). PPK1 from this study would have only 2% of its maximal activity under normal intracellular phosphate concentrations of 3-10 mM reported in *Synechococcus* (Ritchie et al., 1997) grown in BG-11 medium (with phosphate). Moreover, this explains a 30-fold increase in polyphosphate-synthesizing activity reported in phosphate-starved cultures of cyanobacteria (Grillot & Gibson, 1979). This is an example of *phosphate-luxury uptake*, already described in many cyanobacteria and aquatic microorganism and is of high importance for survival in phosphate-poor environments where cells must adapt to rapidly scavenge environmental phosphate, once available (Li & Dittrich, 2019; Solovchenko et al., 2020). *Phosphate-luxury uptake* entails fast transfer of phosphate into the cell in energy dependant-manner and its accumulation in multifold higher amounts compared to normal growth. Hence, PPK1 could serve as a sensor and regulator of cellular Pi levels as it would produce polyphosphate as long as intracellular phosphate remains above certain threshold, provided with ATP as an energy source.

It is therefore very likely that high allosteric dependence on phosphorus of PPK1 activity in *Synechocystis* is a part of *phosphate-luxury uptake* strategy. Therefore, it would be interesting to determine the exact location of the allosteric sites in PPK1 and its conservation among other aquatic microbes. To further confirm the role of PPK1 during *phosphate-luxury uptake*, the rate of phosphate-removal from the media of phosphate-starved cultures of WT and *ppk* should be compared.

As well, this study proved that PPK1 from *Synechocystis* doesn't require polyphosphate as a primer in its reaction of polyphosphate synthesis (**Figure 20**), unlike some other PPK enzymes (Robinson & Wood, 1986).

PPK1 from *Synechocystis* can also degrade polyphosphate while generating ATP from ADP. This reaction is likely of no physiological relevance as it reaches a plateau very soon after its start, even when provided with high concentration of ADP (10 mM) as a substrate (**Figure 21**). As well, the rate of this reaction is not affected by the presence of phosphate. It is more likely that another enzyme, namely PPK2 is responsible for ATP generation from polyphosphate in this organism.

6. CONCLUSION

As a part of this Master Thesis a *ppk* mutant deficient in polyphosphate kinase enzyme has been characterized for the first time in *Synechocystis* and as well for the first time in some species of cyanobacteria.

Lack of polyphosphate doesn't impact growth of *Synechocystis* under normal conditions. Also, polyphosphate doesn't seem to be of huge importance in nitrogen starvation, except maybe for survival during longer periods of starvation. This is best shown by the emergence of adapted normal-resuscitating *ppk* mutant. Whole-genome sequencing of non-adapted and adapted *ppk* mutant will clarify function of polyphosphate in nitrogen starvation and possibly identify a new yet unknown signalling pathway involved in resuscitation from nitrogen chlorosis. On the other hand, lack of polyphosphate seems to disrupt cell's energy metabolism seen in two-fold higher adenylate levels. This probably negatively affects resuscitation from nitrogen chlorosis, most likely by preventing glycogen catabolism.

Secondly, a protocol for absolute quantification of polyphosphate based on phenol-chloroform extraction and ethanol precipitation of polyphosphate followed by its enzymatic degradation has been adapted for this organism.

It was proved that polyphosphate kinase 1 is the only polyphosphate-synthesizing enzyme in *Synechocystis*. It shows similar kinetic parameters in terms of maximum velocity and substrate affinity as the other already characterized PPK enzymes. Further, it displays huge cooperative allosteric dependence of its activity on inorganic phosphate. This observation provides an explanation for physiological and ecological phenomena in which cyanobacteria and other aquatic microorganisms rapidly accumulate huge amounts of polyphosphate after period of phosphate-starvation in a process known as *phosphate-luxury uptake*.

7. REFERENCES

- Agostoni, M., Logan-Jackson, A. R., Heinz, E. R., Severin, G. B., Bruger, E. L., Waters, C. M., Montgomery, B. L. (2018). Homeostasis of second messenger cyclic-di-AMP is critical for cyanobacterial fitness and acclimation to abiotic stress. *Frontiers in Microbiology*, **9**(May), 1–13.
- Ahn, K., Kornberg, A. (1990). Polyphosphate Kinase from *Escherichia coli* Purification and demonstration of a phosphoenzyme intermediate. *Biochemistry*, **265**(20), 11734–11739.
- Akiyama, M., Crooke, E., Kornberg, A. (1993). An exopolyphosphatase of *Escherichia coli*. The enzyme and its ppx gene in a polyphosphate operon. *Journal of Biological Chemistry*, **268**(1), 633–639.
- Ault-Riché, D., Fraley, C. D., Tzeng, C. M., Kornberg, A. (1998). Novel assay reveals multiple pathways regulating stress-induced accumulations of inorganic polyphosphate in *Escherichia coli*. *Journal of Bacteriology*, **180**(7), 1841–1847.
- Baxter, M., Jensen, T. (1980). Uptake of magnesium, strontium, barium, and manganese by *Plectonema boryanum* (Cyanophyceae) with special reference to polyphosphate bodies. *Protoplasma*, **104**(1–2), 81–89.
- Bentley-DeSousa, A., Holinier, C., Moteshareie, H., Tseng, Y. C., Kajjo, S., Nwosu, C., Amodeo, G. F., Bondy-Chorney, E., Sai, Y., Rudner, A., Golshani, A., Davey, N. E., Downey, M. (2018). A Screen for Candidate Targets of Lysine Polyphosphorylation Uncovers a Conserved Network Implicated in Ribosome Biogenesis. *Cell Reports*, **22**(13), 3427–3439.
- Brown, M. R. W., Kornberg, A. (2008). The long and short of it - polyphosphate, PPK and bacterial survival. *Trends in Biochemical Sciences*, **33**(6), 284–290.
- Bru, S., Jiménez, J., Canadell, D., Ariño, J., Clotet, J. (2017). Improvement of biochemical methods of polyP quantification. *Microbial Cell*, **4**(1), 6–15.
- Cano, M., Holland, S. C., Artier, J., Burnap, R. L., Ghirardi, M., Morgan, J. A., Yu, J. (2018). Glycogen Synthesis and Metabolite Overflow Contribute to Energy Balancing in Cyanobacteria. *Cell Reports*, **23**(3), 667–672.
- Choi, S. Y., Park, B., Choi, I. G., Sim, S. J., Lee, S. M., Um, Y., Woo, H. M. (2016). Transcriptome landscape of *Synechococcus elongatus* PCC 7942 for nitrogen starvation responses using RNA-seq. *Scientific Reports*, **6**(July), 1–10.
- Christ, J. J., Willbold, S., Blank, L. M. (2020). Methods for the Analysis of Polyphosphate in the Life Sciences. *Analytical Chemistry*, **92**(6), 4167–4176.
- Damrow, R., Maldener, I., Zilliges, Y. (2016). The multiple functions of common microbial carbon polymers , glycogen and PHB , during stress responses in the non-diazotrophic cyanobacterium *Synechocystis* sp . *Frontiers in Microbiology*, **7**(June), 1–10.
- de Almeida, L. G., Ortiz, J. H., Schneider, R. P., Spira, B. (2015). phoU inactivation in *Pseudomonas aeruginosa* enhances accumulation of ppGpp and polyphosphate. *Applied and Environmental Microbiology*, **81**(9), 3006–3015.
- Docampo, R., Ulrich, P., Moreno, S. N. J. (2010). Evolution of acidocalcisomes and their role in polyphosphate storage and osmoregulation in eukaryotic microbes. *Philosophical Transactions of the Royal Society B: Biological Sciences*, **365**(1541), 775–784.

- Doello, S., Klotz, A., Makowka, A., Gutekunst, K., Forchhammer, K. (2018). A specific glycogen mobilization strategy enables rapid awakening of dormant cyanobacteria from chlorosis. *Plant Physiology*, **177**(2), 594–603.
- Forchhammer, K., Schwarz, R. (2018). Minireview nitrogen chlorosis in unicellular cyanobacteria – a developmental program for surviving nitrogen deprivation. *Environmental Microbiology*, **21**(4), 1173–1184.
- Fraleigh, C. D., Rashid, P. H., Lee, S. S. K., Gottschalk, R., Harrison, J., Wood, P. J., Brown, M. R. W., Kornberg, A. (2007). A polyphosphate kinase 1 (*ppk1*) mutant of *Pseudomonas aeruginosa* exhibits multiple ultrastructural and functional defects. *Proceedings of the National Academy of Sciences of the United States of America*, **104**(9), 3526–3531.
- Freimoser, F. M., Hürlimann, H. C., Jakob, C. A., Werner, T. P., Amrhein, N. (2006). Systematic screening of polyphosphate (poly P) levels in yeast mutant cells reveals strong interdependence with primary metabolism. *Genome Biology*, **7**(11), 1–9.
- Fujisawa, T., Narikawa, R., Maeda, S., Watanabe, S., Kanesaki, Y., Kobayashi, K., Nomata, J., Hanaoka, M., Watanabe, M., Ehira, S., Suzuki, E., Awai, K., Nakamura, Y. (2017). CyanoBase: a large-scale update on its 20th anniversary. *Nucleic Acids Research*, **45**(November), 551–554.
- Gómez-García, M. R., Losada, M., Serrano, A. (2003). Concurrent transcriptional activation of *ppa* and *ppx* genes by phosphate deprivation in the cyanobacterium *Synechocystis* sp. strain PCC 6803. *Biochemical and Biophysical Research Communications*, **302**(3), 601–609.
- Gray, M. J., Jakob, U. (2016). Oxidative Stress Protection by Polyphosphate - New Roles for an Old Player. *Current Opinion in Microbiology*, **24**, 1–6.
- Grillot, J. F., Gibson, J. (1979). Regulation of Phosphate Accumulation in the Unicellular Cyanobacterium *Synechococcus*. *Journal of Bacteriology*, **140**(2), 508–517.
- Guo, Y. L., Mayer, H., Vollmer, W., Dittrich, D., Sander, P., Schultz, A., Schultz, J. E. (2009). Polyphosphates from *Mycobacterium bovis* - Potent inhibitors of class III adenylate cyclases. *FEBS Journal*, **276**(4), 1094–1103.
- Henry, J. T., Crosson, S. (2013). Chromosome replication and segregation govern the biogenesis and inheritance of inorganic polyphosphate granules. *Molecular Biology of the Cell*, **24**(20), 3177–3186.
- Hood, R. D., Higgins, S. A., Flamholz, A., Nichols, R. J., Savage, D. F. (2016). The stringent response regulates adaptation to darkness in the cyanobacterium *Synechococcus elongatus*. *Proceedings of the National Academy of Sciences of the United States of America*, **113**(33), 4867–4876.
- Hsieh, P. C., Shenoy, B. C., Jentoft, J. E., Phillips, N. F. B. (1993). Purification of polyphosphate and ATP glucose phosphotransferase from *Mycobacterium tuberculosis* h37ra: Evidence that Poly(p) and ATP glucokinase activities are catalyzed by the same enzyme. *Protein Expression and Purification*, **4**(1), 76–84.
- Kawai, S., Mori, S., Mukai, T., Suzuki, S., Yamada, T., Hashimoto, W., Murata, K. (2000). Inorganic Polyphosphate/ATP-NAD kinase of *Micrococcus flavus* and *Mycobacterium tuberculosis* H37Rv. *Biochemical and Biophysical Research Communications*, **276**(1), 57–63.
- Klauth, P., Pallerla, S. R., Vidaurre, D., Ralfs, C., Wendisch, V. F., Schoberth, S. M. (2006). Determination of soluble and granular inorganic polyphosphate in *Corynebacterium*

- glutamicum*. *Applied Microbiology and Biotechnology*, **72**(5), 1099–1106.
- Klotz, A., Forchhammer, K. (2017). Glycogen, a major player for bacterial survival and awakening from dormancy. *Future Microbiology*, **12**(2), 101–104.
- Klotz, A., Georg, J., Bučinská, L., Watanabe, S., Reimann, V., Januszewski, W., Sobotka, R., Jendrossek, D., Hess, W. R., Forchhammer, K. (2016). Awakening of a dormant cyanobacterium from nitrogen chlorosis reveals a genetically determined program. *Current Biology*, **26**(21), 2862–2872.
- Klotz, A., Reinhold, E., Doello, S., Forchhammer, K. (2015). Nitrogen starvation acclimation in *Synechococcus elongatus*: redox-control and the role of nitrate reduction as an electron sink. *Life*, **5**(1), 888–904.
- Koch, M., Doello, S., Gutekunst, K., Forchhammer, K. (2019). PHB is produced from glycogen turn-over during nitrogen starvation in *Synechocystis* sp. PCC 6803. *International Journal of Molecular Sciences*, **20**(8), 1–14.
- Kornberg, A., Rao, N. N., Ault-Riché, D. (1999). Inorganic Polyphosphate : a molecule of many functions. *Annual Review of Biochemistry*, **68**, 89–125.
- Kumble, K. D., Ahn, K., Kornberg, A. (1996). Phosphohistidyl active sites in polyphosphate kinase of *Escherichia coli*. *Proceedings of the National Academy of Sciences of the United States of America*, **93**(25), 14391–14395.
- Kuroda, A., Murphy, H., Cashel, M., Kornberg, A. (1997). Guanosine tetra- and pentaphosphate promote accumulation of inorganic polyphosphate in *Escherichia coli*. *Journal of Biological Chemistry*, **272**(34), 21240–21243.
- Kuroda, A., Nomura, K., Ohtomo, R., Kato, J., Ikeda, T., Takiguchi, N., Ohtake, H., Kornberg, A. (2001). Role of inorganic polyphosphate in promoting ribosomal protein degradation by the Lon protease in *E. coli*. *Science*, **293**(5530), 705–708.
- Kusano, S., Ishihama, A. (1997). Functional interaction of *Escherichia coli* RNA polymerase with inorganic polyphosphate. *Genes to Cells*, **2**(7), 433–441.
- Lapina, T., Selim, K. A., Forchhammer, K., Ermilova, E. (2018). The PII signaling protein from red algae represents an evolutionary link between cyanobacterial and Chloroplastida PII proteins. *Scientific Reports*, **790**(8), 1–14.
- Li, J., Dittrich, M. (2019). Dynamic polyphosphate metabolism in cyanobacteria responding to phosphorus availability. *Environmental Microbiology*, **21**(2), 572–583.
- Martin, P., Van Mooy, B. A. S. (2013). Fluorometric quantification of polyphosphate in environmental plankton samples: Extraction protocols, matrix effects, and nucleic acid interference. *Applied and Environmental Microbiology*, **79**(1), 273–281.
- McMeechan, A., Lovell, M. A., Cogan, T. A., Marston, K. L., Humphrey, T. J., Barrow, P. A. (2007). Inactivation of *ppk* differentially affects virulence and disrupts ATP homeostasis in *Salmonella enterica* serovars Typhimurium and Gallinarum. *Research in Microbiology*, **158**(1), 79–85.
- Morgan, H. E., Parmeggiani, A. (1964). Regulation of glycogenolysis in muscle. *The Journal of Biological Chemistry*, **239**(8), 2440–2445.
- Morohoshi, T., Maruo, T., Shirai, Y., Kato, J., Ikeda, T., Takiguchi, N., Ohtake, H., Kuroda, A. (2002). Accumulation of Inorganic Polyphosphate in. *Applied and Environmental Microbiology*, **68**(8), 4107–4110.

- Munévar, N. F. V., de Almeida, L. G., Spira, B. (2017). Differential regulation of polyphosphate genes in *Pseudomonas aeruginosa*. *Molecular Genetics and Genomics*, **292**(1), 105–116.
- Nierzwicki Bauer, S. A., Balkwill, D. L., Stevens, S. E. (1983). Three-dimensional ultrastructure of a unicellular cyanobacterium. *Journal of Cell Biology*, **97**(3), 713–722.
- Nomura, K., Kato, J., Takiguchi, N., Ohtake, H., Kuroda, A. (2004). Effects of inorganic polyphosphate on the proteolytic and DNA-binding activities of Lon in *Escherichia coli*. *Journal of Biological Chemistry*, **279**(33), 34406–34410.
- Pick, U., Rental, M., Chitlaru, E., Weiss, M. (1990). Polyphosphate-hydrolysis - a protective mechanism against alkaline stress? *FEBS Letters*, **274**(1–2), 15–18.
- Pitt, F. D., Mazard, S., Humphreys, L., Scanlan, D. J. (2010). Functional characterization of *Synechocystis* sp. strain PCC 6803 *pst1* and *pst2* gene clusters reveals a novel strategy for phosphate uptake in a freshwater cyanobacterium. *Journal of Bacteriology*, **192**(13), 3512–3523.
- Racki, L. R., Tocheva, E. I., Dieterle, M. G., Sullivan, M. C., Jensen, G. J., Newman, D. K. (2017). Polyphosphate granule biogenesis is temporally and functionally tied to cell cycle exit during starvation in *Pseudomonas aeruginosa*. *Proceedings of the National Academy of Sciences of the United States of America*, **114**(12), 2440–2449.
- Rao, N. N., Gómez-García, M. R., Kornberg, A. (2009). Inorganic polyphosphate: essential for growth and survival. *Annual Review of Biochemistry*, **78**(1), 605–647.
- Rao, N. N., Kornberg, A. (1996). Inorganic polyphosphate supports resistance and survival of stationary-phase *Escherichia coli*. *Journal of Bacteriology*, **178**(5), 1394–1400.
- Rehm, B. H. A. (2010). Bacterial polymers: Biosynthesis, modifications and applications. *Nature Reviews Microbiology*, **8**(8), 578–592.
- Reusch, R. N., Huang, R., Bramble, L. L. (1995). Poly-3-hydroxybutyrate/polyphosphate complexes form voltage-activated Ca^{2+} channels in the plasma membranes of *Escherichia coli*. *Biophysical Journal*, **69**(3), 754–766.
- Ritchie, R. J., Trautman, D. A., Larkum, A. W. D. (1997). Phosphate uptake in the cyanobacterium *Synechococcus* R-2 PCC 7942. *Plant and Cell Physiology*, **38**(11), 1232–1241.
- Rittershaus, E., Baek, S., Sasseti, C. (2013). The normalcy of dormancy. *Cell Host Microbe*, **13**(6), 643–651.
- Robinson, N. A., Wood, H. G. (1986). Polyphosphate Kinase from *Propionibacterium shermanii*. *The Journal of Biological Chemistry*, **261**(11), 4481–4485.
- Rubin, B. E., Huynh, T. A. N., Welkie, D. G., Diamond, S., Simkovsky, R., Pierce, E. C., Taton, A., Lowe, L. C., Lee, J. J., Rifkin, S. A., Woodward, J. J., Golden, S. S. (2018). High-throughput interaction screens illuminate the role of c-di-AMP in cyanobacterial nighttime survival. *PLoS Genetics*, **14**(4), 1–21.
- Savchenko, A., Brown, G., Kochinyan, S., Osipiuk, J., Proudfoot, M., Yakunin, A. F., Evdokimova, E., Joachimiak, A., Nocek, B., Edwards, A. M. (2008). Polyphosphate-dependent synthesis of ATP and ADP by the family-2 polyphosphate kinases in bacteria. *Proceedings of the National Academy of Sciences*, **105**(46), 17730–17735.
- Seki, Y., Nitta, K., Kaneko, Y. (2014). Observation of polyphosphate bodies and DNA during the cell division cycle of *Synechococcus elongatus* PCC 7942. *Plant Biology*, **16**(1), 258–

- Solovchenko, A., Gorelova, O., Karpova, O., Selyakh, I., Semenova, L., Chivkunova, O., Baulina, O., Vinogradova, E., Pugacheva, T., Scherbakov, P., Vasilieva, S., Lukyanov, A., Lobakova, E. (2020). Phosphorus Feast and Famine in Cyanobacteria: Is Luxury Uptake of the Nutrient Just a Consequence of Acclimation to Its Shortage? *Cells*, **9**(9), 1–21.
- Spät, P., Klotz, A., Rexroth, S., Maček, B., Forchhammer, K. (2018). Chlorosis as a developmental program in cyanobacteria: the proteomic fundament for survival and awakening. *Molecular Cell Proteomics*, **17**(9), 1650–1669.
- Sureka, K., Dey, S., Datta, P., Singh, A. K., Dasgupta, A., Rodrigue, S., Basu, J., Kundu, M. (2007). Polyphosphate kinase is involved in stress-induced mprAB-sigE-rel signalling in mycobacteria. *Molecular Microbiology*, **65**(2), 261–276.
- Tumlirsch, T., Sznajder, A., Jendrossek, D. (2015). Formation of polyphosphate by polyphosphate kinases and its relationship to poly(3-hydroxybutyrate) accumulation in *Ralstonia eutropha* strain H16. *Applied and Environmental Microbiology*, **81**(24), 8277–8293.
- Tinsley, C. R., Manjula, B. N., Gotschlich, E. C. (1993). Purification and characterization of polyphosphate kinase from *Neisseria meningitidis*. *Infection and Immunity*, **61**(9), 3703–3710.
- Tzeng, C. M., Kornberg, A. (2000). The multiple activities of polyphosphate kinase of *Escherichia coli* and their subunit structure determined by radiation target analysis. *Journal of Biological Chemistry*, **275**(6), 3977–3983.
- Van De Meene, A. M. L., Hohmann-Marriott, M. F., Vermaas, W. F. J., Roberson, R. W. (2006). The three-dimensional structure of the cyanobacterium *Synechocystis* sp. PCC 6803. *Archives of Microbiology*, **184**(5), 259–270.
- Van Dien, S. J., Keyhani, S., Yang, C., Keasling, J. D. (1997). Manipulation of independent synthesis and degradation of polyphosphate in *Escherichia coli* for investigation of phosphate secretion from the cell. *Applied and Environmental Microbiology*, **63**(5), 1689–1695.
- Varas, M., Valdivieso, C., Mauriaca, C., Ortíz-Severín, J., Paradela, A., Poblete-Castro, I., Cabrera, R., Chávez, F. P. (2017). Multi-level evaluation of *Escherichia coli* polyphosphate related mutants using global transcriptomic, proteomic and phenomic analyses. *Biochimica et Biophysica Acta - General Subjects*, **1861**(4), 871–883.
- Varela, C., Mauriaca, C., Paradela, A., Albar, J. P., Jerez, C. A., Chavez, F. P. (2010). New structural and functional defects in polyphosphate deficient bacteria: A cellular and proteomic study. *BMC Microbiology*, **10**(7), 1–14.
- Voronkov, A., Sinetova, M. (2019). Polyphosphate accumulation dynamics in a population of *Synechocystis* sp. PCC 6803 cells under phosphate overplus. *Protoplasts*, **256**(4), 1153–1164.
- Yu, Y., You, L., Liu, D., Hollinshead, W., Tang, Y. J., Zhang, F. (2013). Development of *Synechocystis* sp. PCC 6803 as a Phototrophic Cell Factory. *Marine Drugs*, **11**, 2894–2916.
- Zhang, H., Ishige, K., Kornberg, A. (2002). A polyphosphate kinase (PPK2) widely conserved in bacteria. *Proceedings of the National Academy of Sciences*, **99**(26), 16678–16683.

APPENDIX

Table S1 - Composition of macroelements and trace elements in BG-11 medium.

BG-11 macroelement	M in 1x BG-11 medium	BG-11 trace element	M in 1x BG-11 medium
NaNO ₃	17.65 mM	H ₃ BO ₃	46.3 μM
K ₂ HPO ₄ x 3 H ₂ O	175.3 μM	MnCl ₂ x 4 H ₂ O	9.2 μM
MgSO ₄ x 7 H ₂ O	304.3 μM	ZnSO ₄ x 7 H ₂ O	0.77 μM
CaCl ₂ x 2 H ₂ O	244.8 μM	Na ₂ MoO ₄ x 2 H ₂ O	1.6 μM
Citric acid & Ferric (III) citrate	31.2 μM	CuSO ₄ x 5 H ₂ O	0.32 μM
	24.5 μM	Co(NO ₃) ₂ x 6 H ₂ O	0.267 μM
EDTA	3.42 μM		
Na ₂ CO ₃	377.4 μM		

All seven macroelements (**Table S1**) were kept as separate 200x stock solutions. Trace elements were kept as single 1000x stock solution that was stored in fridge.

To make 1 l of BG-11 1x medium 5 ml of each macroelement solution was added to 959 ml of miliQ water along with 1 ml of 1000x stock solutions of trace elements. Solution was then autoclaved (121 °C, 20 min) and sterile NaHCO₃ solution was added to a final concentration of 5 mM.

BG-11 agarose plates were made of components from **Table S2**. The mixture was then autoclaved (121 °C, 20 min) and 30 ml of it was poured to a sterile Petri dish.

Table S2 - Composition of medium for BG-11 agarose plates.

component	amount
BG-11 (1x)	500 ml
TES NaOH (1 M, pH 8.2)	2 ml
Bacto-agar	7.5 g
Na ₂ S ₂ O ₃ x 5 H ₂ O	2.4 g

TES buffer: 10 mM Tris, 10 mM EDTA, 0.5% SDS

Table S3 – The list of used primers.

notation	description	sequence (5' - 3')
fw <i>ppk</i> segregation check	binds upstream of <i>ppk</i> gene	AGCTAGCAGTCCCGCCCAAC
rev <i>ppk</i> segregation check	binds downstream of <i>ppk</i> gene	GATCAACCTGATCGCCTATC
rev2 <i>ppk</i> segregation check	binds <i>ppk</i> coding region	TGGTGGCTCCGGTTAATATG
<i>ppk</i> fw ol pET15b	Gibson cloning of <i>ppk</i> into XhoI site of pET15b	GCAGCGGCCTGGTGCCGCGCGGCAGCCATAT GCTCGAGATGATCCAAGCTATGCCCTC
<i>ppk</i> rev ol pET15b	Gibson cloning of <i>ppk</i> into XhoI site of pET15b	CCAACTCAGCTTCCTTTCGGGCTTTGTTAGCA GCCGGATCTCAAACCTGAACGTAGTTCC
fw pET	sequencing of pET	CCGCGAAATTAATACGACTCAC
rev pET	sequencing of pET	CCTCAAGACCCGTTTAGAGG

Table S4 - Gibson assembly master mix.

Aliquots (15 µl):	V/µl
5x Iso Buffer	4.0
miliQ	8.67
1:10 NEB T5 Exonuclease (1 U/µl)	0.08
NEB Q5 DNA polymerase (2 U/µl)	0.25
NEB Taq DNA Ligase (40 U/µl)	2.0

5x Iso Buffer: 500 mM Tris-HCl pH 7.5, 50 mM MgCl₂, 50 mM DTT, 1 mM dNTP, 5mM NAD, 25% PEG-8000

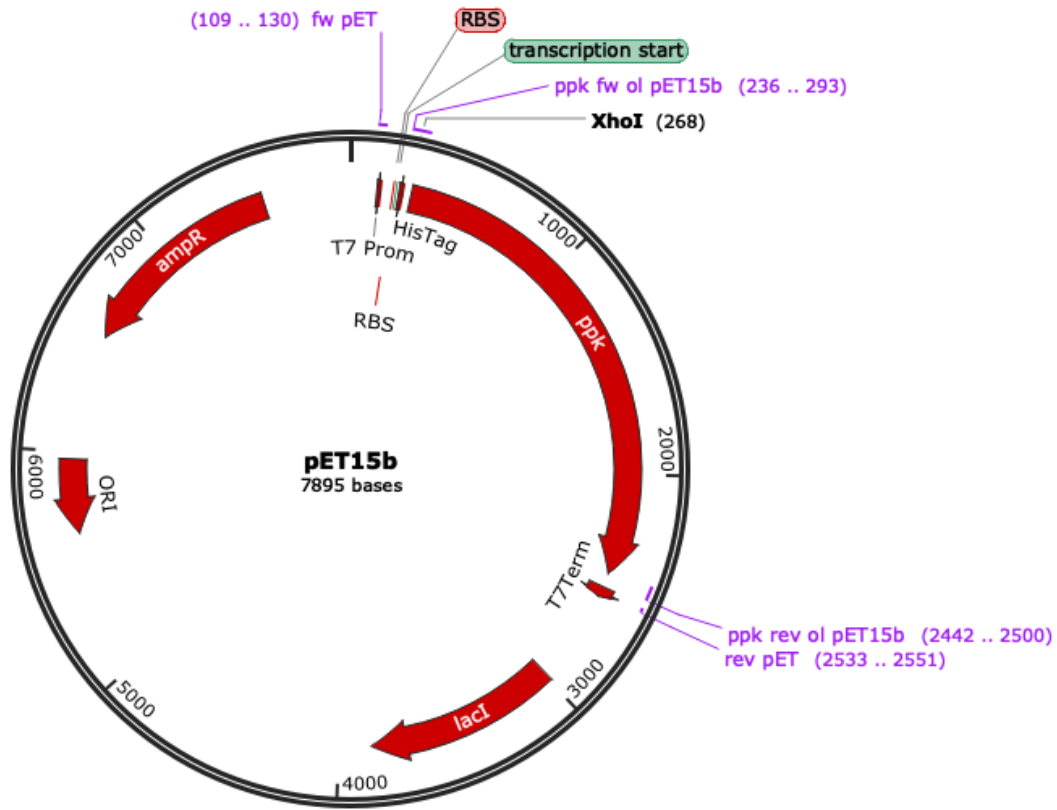
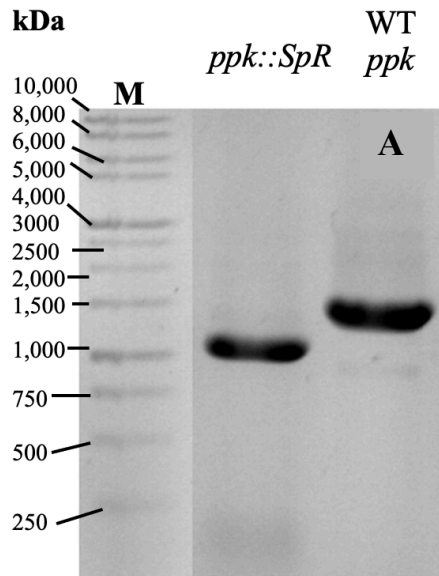
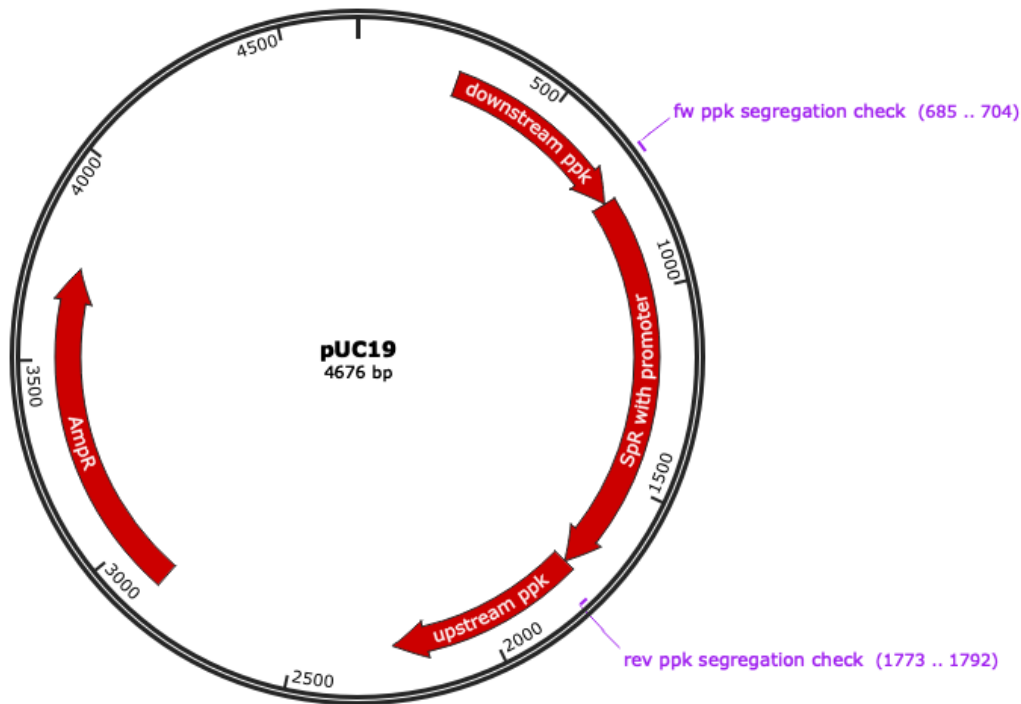


Figure S1 - Plasmid map of pET15b used for cloning and expression of PPK1 protein. Gene *ppk* is inserted in XhoI restriction site by Gibson assembly. ampR - ampiciline resistance, RBS - ribosome binding site, lacI - lac repressor, RBS - ribosome binding site, ORI - origin of replication.



Created with SnapGene®



Created with SnapGene®

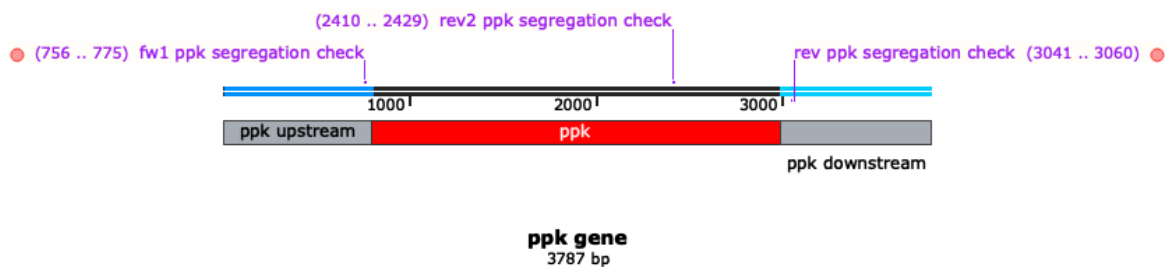


Figure S2 - **A**) Segregation check of *ppk* mutant by colony PCR. M - DNA standard (GenLadder Gennaxon), first lane: *ppk::SpR*, second lane: WT *ppk* gene. **B**) plasmid map of pUC19 plasmid used for knock-out of *ppk* gene with Spectinomycin resistance cassette (SpR) surrounded by upstream and downstream regions of *ppk* gene, ampR - ampiciline resistance **C**) *ppk* gene with binding site for primers used in segregation check by PCR. *ppk::SpR* fragment length - 1107 bp, WT fragment length - 1674 bp.

CURRICULUM VITAE

Ana Janović was born in Zagreb, Croatia in 1996. She graduated from Science High School of Vladimir Prelog in 2015. In the same year she enrolled in the undergraduate programme of Molecular Biology at the Faculty of Science, University of Zagreb. She obtained her Bachelor's degree in 2018 and continued with the Master programme of Molecular Biology at the same faculty. She did student internship with the support of Erasmus grant at the University of Tübingen in Germany in the laboratory of Prof. Dr. Karl Forchhammer in the summer of 2019. There she studied the role of polyphosphate polymer in cyanobacteria *Synechocystis* sp. PCC 6803. She continued with her Master Thesis work in the same lab on the same topic with the support of Erasmus grant.

She speaks English and German language and does Thai-boxing in her spare time.